Mechanics and Materials Center
TEXAS A&M UNIVERSITY
College Station, Texas

AFOSR.TR. 89-1696

AD-A216 095

STUDIES ON DEFORMATION AND FRACTURE OF VISCOELASTIC COMPOSITE MATERIALS

Approved for public release;
distribution unlimited.

FINAL TECHNICAL REPORT

R.A. SCHAPERY

AIR FORCE OFFICE OF SCIENTIFIC RESEARCH
OFFICE OF AEROSPACE RESEARCH
UNITED STATES AIR FORCE
GRANT NO. AFOSR-87-0257

MM 5762-89-14

NOVEMBER 1989

SECURITY CLASSIFICATION OF THIS PAGE

REPORT DOCUMENTATION PAGE

Form Approved
OMB No. 0704-0188

1a. REPORT SECURITY CLASSIFICATION unclassified	1b. RESTRICTIVE MARKINGS
2a. SECURITY CLASSIFICATION AUTHORITY	3. DISTRIBUTION/AVAILABILITY OF REPORT Approved for public release; distribution unlimited.
2b. DECLASSIFICATION/DOWNGRADING SCHEDULE	
4. PERFORMING ORGANIZATION REPORT NUMBER(S) MM-5762-89-14	5. MONITORING ORGANIZATION REPORT NUMBER(S) AFOSR-TR- 89-1696
6a. NAME OF PERFORMING ORGANIZATION Mechanics and Materials Center Texas A&M	6b. OFFICE SYMBOL (If applicable)
6c. ADDRESS (City, State, and ZIP Code) College Station, TX 77843	7a. NAME OF MONITORING ORGANIZATION AFOSR/NA
	7b. ADDRESS (City, State, and ZIP Code) Building 410 Bolling AFB, DC 20332-6448
8a. NAME OF FUNDING/SPONSORING ORGANIZATION AFOSR	8b. OFFICE SYMBOL (If applicable) NA
	9 PROCUREMENT INSTRUMENT IDENTIFICATION NUMBER Grant No. AFOSR-87-0257
8c. ADDRESS (City, State, and ZIP Code) Building 410 Bolling AFB, DC 20332-6448	10. SOURCE OF FUNDING NUMBERS

PROGRAM ELEMENT NO.	PROJECT NO.	TASK NO	WORK UNIT ACCESSION NO.
61102F	2302	B2	

11. TITLE (Include Security Classification) Studies on Deformation and Fracture of Viscoelastic Composite Materials

12. PERSONAL AUTHOR(S)
R.A. Schapery

13a. TYPE OF REPORT	13b. TIME COVERED	14. DATE OF REPORT (Year, Month, Day)	15. PAGE COUNT
Final	FROM 6/15/87 TO 9/14/89	November 1989	10 + Appendix

16. SUPPLEMENTARY NOTATION

17. COSATI CODES			18. SUBJECT TERMS (Continue on reverse if necessary and identify by block number)
FIELD	GROUP	SUB-GROUP	Composites; Fracture of Composites; Damage; Fiber-Reinforced Plastic; Delamination

19. ABSTRACT (Continue on reverse if necessary and identify by block number)

Theoretical and experimental work on the deformation and fracture of structural composite materials is summarized. Research on limited path-independence of work for inelastic laminates under axial and torsional loading and unloading is summarized first. These studies on pure axial loading, pure torsional loading, and combined axial-torsional loading provide support for the theoretically predicted path-independence of work for limited deformation paths. This path-independence is shown to be helpful in the development of simplified methods of deformation and fracture characterization and analysis. Summarized next is research on delamination of multidirectional laminates. It is concerned with (1) delamination testing, (2) moment-curvature testing to obtain the J integral, (3) extensions of the J integral analysis, (4) fractography and delamination in the SEM, and (5) analysis of width effects and crack front curvature effects in the double cantilever specimen.

20. DISTRIBUTION/AVAILABILITY OF ABSTRACT	21. ABSTRACT SECURITY CLASSIFICATION
☐ UNCLASSIFIED/UNLIMITED ☑ SAME AS RPT ☑ DTIC USERS	Unclassified
22a. NAME OF RESPONSIBLE INDIVIDUAL Lt. Col. George Haritos	22b. TELEPHONE (Include Area Code) (202) 767-0463
	22c. OFFICE SYMBOL NA

DD Form 1473, JUN 86 — Previous editions are obsolete. — SECURITY CLASSIFICATION OF THIS PAGE

TABLE OF CONTENTS

1. RESEARCH OBJECTIVE 1

2. ACCOMPLISHMENTS 1

2.1 Overview 1

2.2 A Theory of Mechanical Behavior of Elastic Media with Growing Damage and Other Changes in Structure 2

2.3 A Method For Studying Composites with Changing Damage by Correcting For the Effects of Matrix Viscoelasticity 2

2.4 Thermally-Induced Fracture in Composites 3

2.5 Deformation and Delamination of Inelastic Laminates Under Tensile and Torsional Loading 3

2.6 A Method for Mechanical State Characterization of Inelastic Composite Laminates with Damage 4

2.7 Mechanical Characterization and Analysis of Inelastic Composite Laminates with Growing Damage 4

2.8 Determination of the Mode I Delamination Fracture Toughness of Multidirectional Composite Laminates 5

2.9 Effect of Finite Width on Deflection and Energy Release Rate of an Orthotropic Double Cantilever Specimen 5

2.10 A Technique for Predicting Mode I Energy Release Rates Using A First Order Shear Deformable Plate Theory 6

3. LIST OF AFOSR SPONSORED PUBLICATIONS 6

4. PROFESSIONAL PERSONNEL INFORMATION 8

4.1 List of Professional Personnel 8

4.2 Interactions (coupling activities) of the Principal Investigator 8

5. APPENDIX 10

1. RESEARCH OBJECTIVE

The overall objective of the proposed research is to develop and verify mathematical models of deformation and delamination of elastic and viscoelastic fibrous composites with distributed damage. Emphasis of the theoretical and experimental studies is on graphite/epoxy composites under complex loadings which produce matrix damage and delamination.

2. ACCOMPLISHMENTS

2.1 Overview

Methods of deformation and fracture characterization are simplified when strain energy-like potentials based on mechanical work can be used. Research during the grant period has been primarily concerned with development of the theoretical basis for the approach, and with experimental studies which demonstrate its validity for rubber-toughened and untoughened graphite/epoxy composites with growing or constant matrix damage and delamination.

In the following sections the research work and primary findings are summarized by abstracting the papers and dissertations which detail the studies. In Section 2.2 the general theory is covered; it allows for evolving or constant damage. Viscoelastic effects in the matrix with constant damage are considered in Section 2.3 in a study of tubes under axial and torsional loading. Section 2.4 discusses predictions of matrix damage due to thermal stresses and an experimental program that supports the theory. An extensive experimental study of bars under axial and torsional loading is described in Section 2.5; path-independence of work during periods of growing damage is shown for composites with toughened and untoughened resins. Sections 2.6 and 2.7 cover predictions and experimental verification for in-plane loading of laminates; the method of analysis, which is based on a work-potential and its

minimization, is compared in the former study to a method of analysis based on plasticity theory. The work-potential provides the basis for the J-integral in delamination fracture analysis. Investigations using this type of analysis and experimental studies of the double cantilever beam with multidirectional plys is summarized in Section 2.8. Two related studies of beam-width effects and shear deformation effects are described in Sections 2.9 and 2.10, respectively.

The Appendix contains the two papers which appeared after the annual report was submitted in August 1988.

2.2 A Theory of Mechanical Behavior of Elastic Media with Growing Damage and Other Changes in Structure [1]*

Strain energy-like potentials are used to model the mechanical behavior of linear and nonlinear elastic media with changing structure, such as micro- and macrocrack growth in monolithic and composite materials. Theory and experiment show that the applied work for processes in which changes in structure occur is in certain cases independent of some of the deformation history. Consequences of this limited path-independence are investigated, and various relationships for stable mechanical response are derived. For example, it is shown that work is a minimum during stable changes in structure, which should be useful for developing approximate solutions by variational methods. Some final remarks indicate how the theory may be extended to include thermal, viscoelastic, and fatigue effects.

2.3 A Method For Studying Composites with Changing Damage by Correcting For the Effects of Matrix Viscoelasticity [2]

A technique is described for modifying stress-strain data on fibrous composites so that effects of changing damage may be observed without the

*The number in brackets refers to the publication which is abstracted here; the publication list starts on page 6.

complicating effects of matrix viscoelasticity. The method, which is based on micromechanical considerations, reduces the behavior to that of an equivalent elastic composite with damage. The fibers are assumed to be continuous and linearly elastic. The theoretical basis is developed and then the method is illustrated using results from cyclic axial-torsional loading of tubular specimens of graphite/epoxy laminates.

2.4 Thermally-Induced Fracture in Composites [3]

This work is an experimental and analytical investigation of thermally-induced cracking in cross-ply graphite/epoxy composites. It is shown experimentally that both rates and amplitudes of the thermal excursions affect the extent and the form of damage. The analytical study shows that the early stages of sufficiently slow thermal excursions result in crack patterns that are analogous to mechanical loading effects, and can be assessed by an approximate, two-dimensional micro-cracking model. However, three-dimensional aspects of the spatially non-uniform stress field may have to be included to model crack formation under subsequent temperature excursions or rapid thermal fluctuations. In the latter cases oblique and curved cracks develop and the laminate is susceptible to internal and free-edge delaminations.

2.5 Deformation and Delamination of Inelastic Laminates Under Tensile and Torsional Loading [4,5]

This study is a fundamental examination of the theoretical hypothesis that mechanical work is a (multivalued) potential function which characterizes the deformation and fracture behavior of inelastic materials during damage growth processes. Experimental data from fiber-reinforced plastic laminates (with and without rubber particle toughening) subjected to axial and torsional deformation are analyzed for the existence of the work potential. The work

potential is first employed to analyze data from proportional deformation tests and make predictions of load response. Good agreement is obtained between theory and experiment. Data from nonproportional deformation tests are then evaluated for displacement-path independence of work and load response. Domains of path independence are found from specimens strained well into the range of nonlinear inelastic behavior. Thus, the results of these experimental studies support the existence of a work potential. Although viscoelastic effects are present, they are minimized by using isochronal data in the characterization of mechanical work. Finally, work potential theory and experimental results are used to determine critical energy release rates for mixed mode delamination of laminates subjected to axial and torsional deformations.

2.6 A Method for Mechanical State Characterization of Inelastic Composite Laminates with Damage [6]

The method using a work potential, and its minimization, is described for the characterization of mechanical behavior of inelastic composites with damage, but without significant time-dependent behavior. It is based on the theoretically and experimentally motivated assumption of path-independence of mechanical work over limited ranges of stress or strain states. This method and, for comparison, an approach employing plasticity theory are illustrated with the special case of a unidirectional-fiber laminate or ply. Use of the work-potential method for a multidirectional-fiber laminate is discussed in the concluding remarks.

2.7 Mechanical Characterization and Analysis of Inelastic Composite Laminates with Growing Damage [7]

A method of laminate characterization and analysis is described in which

growing damage and other inelastic phenomena are treated using the same mathematical formalism, thus simplifying the description of mechanical response. It is based on the observation that the applied work is not sensitive to many details of the deformation history. Following a brief discussion of the thermodynamically-based theory, a special version is used along with experimental data on graphite/epoxy composite to obtain an explicit mathematical characterization of a unidirectional ply. Predictions of mechanical response are then compared to experimental results for a variety of layups, one of which delaminates from the edges. Good agreement between theory and experiment is shown.

2.8 Determination of the Mode I Delamination Fracture Toughness of Multidirectional Composite Laminates [8]

The objective of this study is to develop and verify a J-integral method for characterizing mode I delamination fracture of composite laminates with distributed matrix damage. Attention focuses on the special problems associated with delamination of composites with multidirectional (as opposed to unidirectional) layups. Nonlinear beam theory is used to analyze the double cantilever beam specimen to derive an approximate expression for the J-integral. A related test method is proposed. An experimental program and results are described which explore the utility of the method and the variables affecting delamination of multidirectional composites.

2.9 Effect of Finite Width on Deflection and Energy Releases Rate of an Orthotropic Double Cantilever Specimen [9]

The problem of an orthotropic cantilevered plate subjected to a uniformly distributed end load is solved by the Rayleigh-Ritz energy method. The result is applied to laminated composite, double cantilevered specimens to estimate

the effect of crack tip constraint on the transverse curvature, deflection and energy release rate. The solution is also utilized to determine finite width correction factors for fracture energy characterization tests in which neither plane stress nor plane strain conditions apply.

2.10 A Technique for Predicting Mode I Energy Release Rates Using A First Order Shear Deformable Plate Theory [10]

Utilizing a first order shear deformable plate theory, a technique is described for predicting the distribution of the energy release rate along a curved or straight mode I planar crack in the plane of a plate (such as a delamination crack). Accuracy of the technique is assessed by comparing the distributions of energy release rate with those predicted by two and three dimensional finite element analyses of double cantilever beam specimens with straight crack fronts.

3. LIST OF AFOSR SPONSORED PUBLICATIONS

[1]. R.A. Schapery, "A Theory of Mechanical Behavior of Elastic Media with Growing Damage and Other Changes in Structure," To be published in J. Mechanics and Physics of Solids, 1989. Texas A&M Univ. Report MM 5762-88-1 (1988).

[2]. R.D. Tonda and R.A. Schapery, "A Method for Studying Composites with Changing Damage by Correcting for the Effects of Matrix Viscoelasticity," Damage Mechanics in Composites. A.S.D. Wang and G.K. Haritos, Eds., AD-Vol 12, American Society of Mechanical Engineers, N.Y., 45-51 (1987).

[3]. G.P. Fang, R.A. Schapery and Y. Weitsman, "Thermally Induced Fracture in Composites" Engineering Fracture Mechanics, Vol. 33, 619-632 (1989). (A portion of this research was supported by an AFOSR grant

with Dr. Y. Weitsman as principal investigator.)

[4]. M.J. Lamborn, "Deformation and Delamination of Inelastic Laminates Under Tensile and Torsional Loading," Ph.D. Dissertation, Texas A&M Univ., Dec. 1989. Texas A&M Univ. Report No. MM 5762-89-15 (1989).

[5]. M.J. Lamborn and R.A. Schapery, "An Investigation of Deformation Path-Independence of Mechanical Work in Fiber-Reinforced Plastics," Proc. 4th Japan-U.S. Conference on Composite Materials, 991-997 (1988).

[6]. R.A. Schapery, "A Method for Mechanical State Characterization of Inelastic Composite Laminates with Damage", Advances in Fracture Research, Proc. Seventh Int. Conf. Fracture, Vol. 3, 2177-2189 (1989).

[7]. R.A. Schapery, "Mechanical Characterization and Analysis of Inelastic Composite Laminates with Growing Damage," Mechanics of Composite Materials and Structures, ASME AMD-Vol. 100, 1-9 (1989).

[8]. D.P. Goetz, "Determination of the Mode I Delamination Fracture Toughness of Multidirectional Composite Laminates," Ph.D. Dissertation, Dec. 1988. Texas A&M Univ. Report No. MM 5762-89-5 (1989). (A portion of this research was supported by an AFOSR grant with Dr. W.L. Bradley as principal investigator.)

[9]. B.D. Davidson, and R.A. Schapery, "Effect of Finite Width on Deflection and Energy Release Rate of a Orthotropic Double Cantilever Specimen," J. Composite Materials, Vol. 22, 640-656 (1988). (Dr. Davidson's contribution was sponsored by NASA).

[10]. B.D. Davidson and R.A. Schapery," A Technique for Predicting Mode I Energy Release Rates Using a First-Order Shear Deformable Plate Theory," To be published in Engineering Fracture Mechanics, 1989. (Dr. Davidson's contribution was sponsored by NASA).

4. PROFESSIONAL PERSONNEL INFORMATION

4.1 List of Professional Personnel

Richard Schapery, Principal Investigator

Douglas Goetz, Graduate Research Assistant
Awarded Ph.D. in Mechanical Engineering, Dec. 1988.

Mark Lamborn, Graduate Research Assistant
To be Awarded Ph.D. in Civil Engineering, Dec. 1989.

Bob Harbert, Assistant Research Engineer
(Laboratory Staff Member)

Carl Fredericksen, Electronics Technician
(Laboratory Staff Member)

4.2 Interactions (coupling activities) of the Principal Investigator

Spoken Papers and Lectures

1. Paper given at Engineering Science Conference, Univ. of Utah (Sept. 1987): "On the Mechanics of Crack Closing and Bonding in Viscoelastic Media".

2. Paper on overview of research on four AFOSR Grants to Texas A&M at DOD/NASA Composites Review Meeting (Oct. 1987): "Some Damage Models for Composites".

3. Paper given at ASME Annual Winter Meeting, Boston (Dec. 1987): "A Method for Studying Composites with Changing Damage by Correcting for the Effects of Matrix Viscoelasticity".

4. Lecture at Adhesion Society Meeting, Charleston, S.C. (Feb. 1988): "Viscoelastic Effects and Fracture of Adhesive Joints".

5. Paper given at IUTAM Conference on Nonlinear Fracture Mechanics, Caltech (March 1988): "On Some Path-Independent Integrals and Their Use in Fracture of Nonlinear Viscoelastic Media."

6. Paper given at ASTM Symposium on Composite Materials, Reno (April 1988): "Constant Rate, Creep Behaviour and the Analysis of Thermoplastic Composites".

7. Lecture at RPI (May 1988): "Some Damage Models for Composite Materials".

8. Lecture at B.F. Goodrich (Nov. 1988): "Viscoelastic Behavior of Composite Materials".

9. Lecture at the University of Texas (March 1989): "Analysis of

Composite Laminates with Damage".

10. Paper given at the Seventh International Conference on Fracture (March 1989): "A Method for Mechanical State Characterization of Inelastic Composite Laminates With Damage".

11. Lecture at the University of Illinois, National Center for Composite Materials Research (April 1989): "Mechanical Characterization and Analysis of Inelastic Composite Laminates With Damage".

12. Paper given at the Third ASCE/ASME Joint Mechanics Conference, La Jolla (July, 1989): "Mechanical Characterization and Analysis of Inelastic Composite Laminates with Growing Damage".

13. Lecture at Kirtland Air Force Base (August 1989): "Damage Mechanics of Composite Materials".

14. Paper given at IUTAM Conference on Ice Mechanics, St. Johns, Newfoundland (August 1989): "Models for Deformation Behavior of Viscoelastic Media with Distributed Damage and Their Applicability to Ice".

15. Lecture at the Southwest Research Institute (Sept. 1989): "Path Independent Integrals for Nonlinear Viscoelastic Media".

Additional Coupling Activities

1. Member on National Academy of Sciences committee: "Energy Conversion" (Nov. 1987).

2. Lecturer in short course at Israel Aircraft Industries, Tel Aviv (Dec. 1987): "Damage Tolerance of Composite materials."

3. Member of NASA Advisory Panel on High-Altitude Balloons (1988-present).

4. Session chairman at four conferences.

APPENDIX

1. A Metnod for Mechanical State Characterization of Inelastic Composite Laminates With Damage.
2. Mechanical Characterization and Analysis of Inelastic Composite Laminates with Growing Damage.

Report No. MM 5762-88-10
August, 1988 (Rev. 9-88)

A METHOD FOR MECHANICAL STATE CHARACTERIZATION OF INELASTIC COMPOSITE LAMINATES WITH DAMAGE*

R. A. SCHAPERY

Department of Civil Engineering, Texas A&M University,
College Station, Texas 77843

ABSTRACT

A method using a work potential is described for the characterization of mechanical behavior of inelastic composites with damage, but without significant time-dependent behavior. It is based on the theoretically and experimentally motivated assumption of path-independence of mechanical work over limited ranges of stress or strain states. This method and, for comparison, an approach employing plasticity theory are illustrated with the special case of a unidirectional-fiber laminate or ply. Use of the work-potential method for a multidirectional-fiber laminate is discussed in the concluding remarks.

KEYWORDS

Composites, Laminates, Damage, Inelasticity, Plasticity

1. INTRODUCTION

Considerable progress has been made in recent years on the development of high strength-to-weight, tough structural composites. This behavior is achieved in-part by laminating individual plies of unidirectional, continuous fiber-reinforced plastic or metal. The laminates are resistant to crack growth through the thickness if two or more fiber orientations are used. Delamination and cracking within plies is reduced by using ductile matrices. For organic polymer matrices, the ductility is obtained by adding toughening agents, such as rubber particles, to normally brittle crosslinked resins, or by using resins with little or no crosslinking (Johnston, 1987). These improvements in material performance place increased demands on the structural designer and those concerned with the micromechanics of composites if inelasticity is due to both plastic deformation and damage or if it has to be considered under a wider range of conditions than for the brittle matrix systems.

Traditionally, matrix ductility has been treated using incremental plasticity theory (Christensen, 1979) while micro- and macrocracking of composites have been analyzed using linear elasticity theory (Wang and

*Published in Advances in Fracture Research, Proc. Seventh Int. Conf. Fracture, Vol. 3, 2177-2189, 1989.

Haritos, 1987). In this paper we discuss an approach to characterizing inelastic composite material behavior which is based on total rather than incremental strains. Also, the approach uses the same mathematical formalism for inelasticity due to plastic deformation as due to cracking on various scales and other damage mechanisms; the term inelasticity, as used here, refers to any stable behavior in which stress or load is not always a single-valued function of strain or displacement. It is believed that this unified approach simplifies the problem of understanding and predicting mechanical behavior of composites with damage. Fatigue and time-dependent behavior and thermal effects are not treated here, although approaches have been proposed in the papers which motivated the present study (Schapery, 1987a, 1988).

Schapery (1987a) has shown theoretically that the stresses and mechanical work of deformation are often independent of many details of the deformation history when the inelasticity is due to micro- and macrocracking. However, cracking is not the only mechanism that produces this behavior. Indeed, it has been observed for a rubber-toughened, graphite/epoxy composite in which there are probably significant effects of shear banding in the matrix (possibly initiated or enhanced by cavitation of rubber particles) (Yee, 1987). This limited path-independence was used by Schapery (1988) to develop a constitutive theory that treats different inelastic mechanisms within the same mathematical framework. Also, as shown by Schapery (1987a), fracture analysis is simplified when this theory is valid because of the applicability of certain equations for relating changes in local and global energies.

Figure 1 illustrates one type of path-independence we have found for the rubber-toughened composite. Rectangular composite bars with an angle-ply layup (alternating fiber angle, $\theta = \pm 35^{\circ}$, with respect to the axial direction) were subjected to various axial and torsional deformations

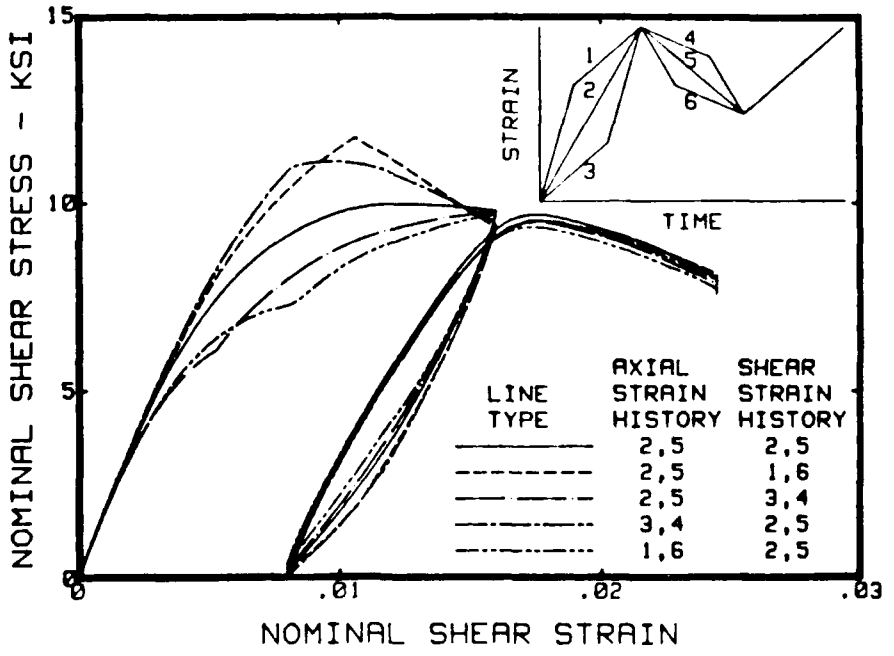

Fig. 1. Shear stress-strain curves for proportional and nonproportional straining of an angle-ply laminate; Hexcel T2C 145/F155 graphite/epoxy $[+-35^{\circ}]_{6S}$; 0.15" thick X 0.5" wide X 8.75" long. From Lamborn and Schapery (1988).

through controlled movement of the end-grips. The different deformation paths are identified in Fig. 1 by number; for example, the bottom line type is used for axial history 1 during the first loading period and axial history 6 during unloading, while the corresponding torsional histories are 2 and 5. The "nominal" shear stress and shear and axial strains are quantities which are proportional to the torque, twist, and axial displacement, respectively; the proportionality coefficients depend only on the specimen dimensions, and are introduced to minimize the effect of specimen-to-specimen size differences.

At the end of the first loading period, the five different strain paths result in practically the same stress (Fig. 1) and total work. The same behavior holds for the unloading and reloading. In contrast, unreinforced aluminum bars exhibit significant path-dependence (Lamborn and Schapery, 1988); we do not know if fiber-reinforced aluminum would exhibit less path-dependence.

Unloading and reloading behavior of the graphite/epoxy material under pure axial or torsional straining is similar to that shown in Fig. 1; there is significant hysteresis and the average slope of the loop decreases with increasing strain at the unloading point. The stress during loading does not usually exhibit a maximum point prior to fracture, in contrast to that in Fig. 1. We are now investigating the damage state as a function of deformation history using similar specimens; significant edge delaminations have been found at the highest stresses for deformation histories like those in Fig. 1.

The primary effects of deformation history on the composite appear to be associated with the sign of (nominal) strain rate and the strain magnitude when the sign last changed. Although a more precise definition of limited path-independence was given by Schapery (1988) here we shall just refer to differences between loading, unloading, and reloading curves, and suppose that for each case there is no effect of path (which is approximately true for the data in Fig. 1).

The local stresses and strains (as opposed to the "nominal" quantities in Fig. 1) are distributed very nonuniformly throughout the specimens used in these axial-torsional tests, and thus the results cannot be used directly in a basic material characterization of the composite. However, it is unlikely that the specimens' overall behavior would exhibit limited path-independence if the ply-level constitutive equations did not reflect this type of behavior.

The discussion in Sections 2-4 is concerned primarily with the characterization of the behavior of a undirectional-fiber laminate consisting of one or more plies under the assumption of this limited path-independence. Special versions of the theory (Schapery, 1988) are used here to illustrate it for composites. Specifically, Section 2 considers nonlinear loading and unloading behavior, and expresses the inelasticity in terms of one parameter S which represents the effect of microstructural changes on the overall stress-strain behavior; such S-parameters provide the inelasticity and, in the context of some thermodynamic formulations, are called internal state variables. Section 3 contrasts the theory with a plasticity model based on the normality rule, and uses the characterization in Section 2 as an example. In Section 4 another illustration is given by using a linear approximation for unloading behavior. Concluding remarks in Section 5 discuss in-part the use of unidirectional ply characterization in laminates with ply-level and larger scales of damage.

2. A CONSTITUTIVE EQUATION WITH NONLINEAR UNLOADING BEHAVIOR

Figure 2 shows a unidirectional laminate or ply and the coordinate notation, in which the x_1 axis is parallel to the fibers; the x_3 axis is normal to the ply plane. The stresses σ_i and strains ε_i ($i = 1,2,\ldots 6$) are mechanical variables referred to the principal material coordinates x_i. In most of the discussion it will be convenient to use this single index notation. As is customary, $i = 4,5,6$ are used for the shearing variables; the relationship between single and double indexed variables for plane stress is

$$\begin{aligned} \sigma_{11} &= \sigma_1, \quad \sigma_{22} = \sigma_2, \quad \sigma_{12} = \sigma_6 \\ \varepsilon_{11} &= \varepsilon_1, \quad \varepsilon_{22} = \varepsilon_2, \quad 2\varepsilon_{12} = \varepsilon_6 \end{aligned} \tag{1}$$

A constitutive equation will be proposed which accounts for nonlinear loading and unloading behavior and which is consistent with the path-independence of work discussed in the Introduction as well as the nonlinear behavior reported by Lou and Schapery (1971) and Sun and Chen (1987); the reader is referred to these two papers for the experimental data, as space does not permit its reproduction here. Specifically, a strain energy density $w = w(\varepsilon_i, S)$ is assumed to exist, where the microstructure state is defined by S; only one structure parameter S will be used here, although more could be introduced, if necessary. By definition of w,

$$\sigma_i = \partial w / \partial \varepsilon_i \tag{2}$$

In both aforementioned references strains are expressed in terms of stresses, and thus it is helpful to eliminate w in favor of a so-called dual strain energy density $w_\sigma = w_\sigma(\sigma_i, S)$,

$$w_\sigma \equiv w - \sigma_i \varepsilon_i \tag{3}$$

(Throughout this paper the summation convention is employed, in which a repeated index implies summation over its range.) By using (2) and introducing differential changes in (3), it follows in the usual way that

$$\varepsilon_i = - \partial w_\sigma / \partial \sigma_i \tag{4}$$

A form of w_σ discussed by Schapery (1988, Eq. (A24)) is proposed now for characterizing ply behavior,

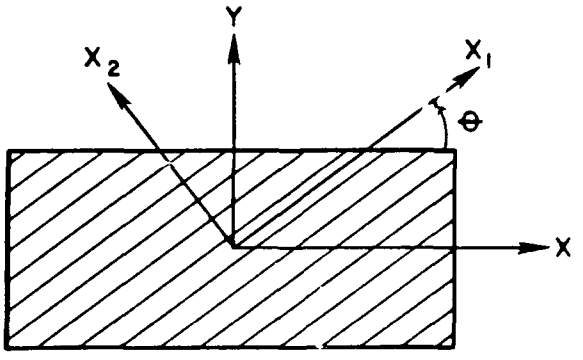

Fig. 2. Unidirectional composite and coordinates.

$$w_\sigma = w_{\sigma o} + P(\sigma_o, S) \tag{5}$$

where $w_{\sigma o} = w_{\sigma o}(\sigma_i)$, $\sigma_o = \sigma_o(\sigma_i)$, and P are presently arbitrary functions. The mechanical work during processes in which S changes can be shown to be independent of path if and only if $S = S(\sigma_o)$. ; proof of this statement may be made by the same method as used in a study of w (Schapery, 1988, Appendix A). The function $S(\sigma_o)$ can be absorbed in the functional dependence of P on S, and thus we may use $S = \sigma_o$ whenever S changes without any actual limitation in the model. Whether S^o varies or is constant, the strains are obtained from (4) and (5),

$$\varepsilon_i = \varepsilon_i^e - \frac{\partial P}{\partial \sigma_o} \frac{\partial \sigma_o}{\partial \sigma_i} \tag{6}$$

where, by definition,

$$\varepsilon_i^e \equiv - \partial w_{\sigma o}/\partial \sigma_i \tag{7}$$

The ε_i^e are defined through derivatives of a fully path-independent potential, $w_{\sigma o}$, and thus it is appropriate to call them "elastic strains". All stress-history effects are in the second term in (6), which gives the "inelastic strains".

In order to obtain a constitutive equation that agrees with Sun and Chen's experimental data we select for σ_o the quadratic form,

$$\sigma_o = (a_{ij}\, \sigma_i\, \sigma_j)^{\frac{1}{2}} \tag{8}$$

where the a_{ij} are constants; as the antisymmetric components of a_{ij} have no effect on σ_o, we may suppose $a_{ij} = a_{ji}$. Now,

$$\partial \sigma_o/\partial \sigma_i = a_{ij}\, \sigma_j /\sigma_o \tag{9}$$

and thus from (6),

$$\varepsilon_i = \varepsilon_i^e - \frac{\partial P}{\partial \sigma_o} a_{ij}\, \sigma_j /\sigma_o \tag{10}$$

During structure-change processes $S = \sigma_o$, as noted previously, and therefore the coefficient $\partial P/\partial \sigma_o$ depends on only σ_o. For such processes we may thus write

$$\varepsilon_i = \varepsilon_i^e + \varepsilon_o\, a_{ij}\, \sigma_j /\sigma_o \tag{11}$$

where

$$\varepsilon_o = \varepsilon_o(\sigma_o) \equiv -(\partial P/\partial \sigma_o) \text{ evaluated at } S = \sigma_o \tag{12}$$

In the terminology of plasticity theory, (11) is for "loading" processes.

Without fiber fracture, the strain in the fiber direction is essentially independent of stress history in most structural composites; thus, as assumed by Sun and Chen, $a_{1j} = a_{j1} = 0$. We suppose further that the composite is orthotropic, regardless of stress-history, where the axes x_i are the principal material axes; this condition implies the only a_{ij} which do not vanish are a_{22}, a_{23}, a_{33}, a_{44}, a_{55}, a_{66}, as well as $a_{32}(=a_{23})$. There are really only five independent constants because σ_o may be normalized with respect to a constant without limiting the generality of (5); this normalization will be done by simply letting $a_{22} = 1$. If all stresses

vanish except for σ_2, (8) reduces to $\sigma_o = |\sigma_2|$; thus σ_o becomes the applied stress for the case of uniaxial tensile loading normal to the fibers.

For plane stress, $\sigma_3 = \sigma_4 = \sigma_5 = 0$, so that (8) reduces to

$$\sigma_o = (\sigma_2^2 + a_{66}\,\sigma_6^2)^{\frac{1}{2}} \tag{13}$$

From (11),

$$\varepsilon_1 = \varepsilon_1^e \tag{14}$$

$$\varepsilon_2 = \varepsilon_2^e + \varepsilon_o \sigma_2/\sigma_o \tag{15}$$

$$\varepsilon_6 = \varepsilon_6^e + a_{66}\,\varepsilon_o \sigma_6/\sigma_o \tag{16}$$

For uniaxial tension normal to the fibers, $\sigma_o = \sigma_2$, as noted previously. Equation (15) then shows that ε_o reduces to the inelastic component of ε_2. For general stress states ε_o is at most a function of σ_o, according to (12).

By introducing some additional specializations, including the assumption that the ε_i^e are linear in the σ_i, we will finally arrive at Sun and Chen's findings for uniaxial loading of unidirectional, rectangular specimens. Namely, for loading in the x direction (cf. Fig. 2),

$$\sigma_1 = \cos^2\theta\,\sigma_x, \quad \sigma_2 = \sin^2\theta\,\sigma_x, \quad \sigma_6 = -\sin\theta\cos\theta\sigma_x \tag{17}$$

where σ_x is the applied force/area. The axial strain ε_x may be expressed in terms of the strains in (14)-(16) using the second-order tensor transformation rule,

$$\varepsilon_x = \cos^2\theta\,\varepsilon_1 + \sin^2\theta\,\varepsilon_2 - \sin\theta\cos\theta\,\varepsilon_6 \tag{18}$$

Substitution of (14)-(17) into (18) yields

$$\varepsilon_x = \varepsilon_x^e + h^2 \varepsilon_o\,\sigma_x/\sigma_o \tag{19}$$

where ε_x^e is the elastic axial strain, and

$$h \equiv (\sin^4\theta + a_{66}\sin^2\theta\cos^2\theta)^{\frac{1}{2}} \tag{20}$$

Observe also from (13) and (17) that

$$\sigma_o = h\sigma_x \tag{21}$$

We can obtain the function $h(\theta)$ used by Sun and Chen by multiplying (20) by $\sqrt{3}/2$. Equation (19) is the same as derived by them from a plasticity model for loading behavior; this model will be discussed in Section 3.

Experimental information on $\varepsilon_x - \sigma_x$ behavior for two fiber angles θ may be used with (19) to evaluate a_{66} and the function $\varepsilon_o = \varepsilon_o(\sigma_o)$. (Alternatively, one may use data from several fiber angles to determine the a_{66} which minimizes the data spread in the $\varepsilon_o(\sigma_o)$ plot.) Results from tests at other fiber angles then serve to check (19). A simple power law

$$\varepsilon_o = A\,\sigma_o^n \tag{22}$$

where A and n are positive constants, was reported by Sun and Chen to fit

the data out to specimen failure ($\varepsilon_x \simeq 1\%$); for a boron/aluminum composite $n = 5.8$ and $a_{66} = 4$, whereas for graphite/epoxy $n = 3.7$ and $a_{66} = 2.5$. (The constant a_{66} used by Sun and Chen is one-half of the a_{66} used here.) Values of $a_{66} = 4$ and $n = 2.4$ have been obtained recently by Mignery and Schapery (1988) from studies of unidirectional and angle-ply laminates of the same rubber-toughened graphite/epoxy material used to develop the curves in Fig. 1. Although the latter exponent ($n = 2.4$) is smaller than that reported by Sun and Chen for an untoughened unidirectional graphite/epoxy material ($n = 3.7$), the angle-ply stress-strain curves (Mignery and Schapery, 1988) exhibit a larger degree of nonlinearity because the total axial strain range is approximately 5%, as compared to 1% in the former study.

In the much earlier work of Lou and Schapery (1971) it was found that the parameter σ_0 in (13) accounted for the effect of stress state on the functions used to characterize nonlinear viscoelastic behavior of a glass/epoxy composite. The motivation for the use of this parameter came in part from the observation that the octahedral shear stress τ_{oct} can normally be used to correlate multiaxial yielding of plastics (just as for metals). As a simplification, the matrix was viewed as a uniformly stressed layer of material sandwiched between layers of rigid fiber material; i.e., the lines in Fig. 2 at the angle θ were imagined to define layers rather than fibers. Using the principal material axes, Fig. 2, this shear stress is

$$\tau_{oct} = \frac{1}{3}[(\bar{\sigma}_1 - \bar{\sigma}_2)^2 + (\bar{\sigma}_2 - \bar{\sigma}_3)^2 + (\bar{\sigma}_3 - \bar{\sigma}_1)^2 + 6(\bar{\sigma}_4^2 + \bar{\sigma}_5^2 + \bar{\sigma}_6^2)]^{\frac{1}{2}} \qquad (23)$$

where the $\bar{\sigma}_i$ in this equation are the stresses in a matrix layer.

For a matrix in plane stress $\bar{\sigma}_2$ and $\bar{\sigma}_6$ are the same as the stresses σ_2 and σ_6 acting on a composite consisting of parallel layers of matrix and reinforcement material. A factor ν_e was also introduced, as defined by the relationship $\bar{\sigma}_1 = \nu_e \sigma_2$. For a linear elastic, isotropic matrix ν_e is the Poisson's ratio, and for an incompressible elastic or rigid-plastic matrix $\nu_e = 0.5$. Use of these idealizations in (23) yields

$$\tau_{oct} = (2/3c)^{\frac{1}{2}} (\sigma_2^2 + c\sigma_6^2)^{\frac{1}{2}} \qquad (24a)$$

where

$$c = 3/(1 - \nu_e + \nu_e^2) \qquad (24b)$$

As reported by Lou and Schapery (1971) a finite element analysis of a linear elastic composite with a square array of fibers was made to predict the average octahedral shear stress in the matrix. Apart from a numerical factor, (24) was found to be a fairly good approximation to this average. Considering c to be the arbitrary constant a_{66}, it is seen that (24a) and (13) are equivalent parameters for characterizing nonlinear behavior. It is also of interest to find from (24b) that $c = 4$ when $\nu_e = \frac{1}{2}$ and $c = 3.88$ when $\nu_e = 0.35$; the former value is the same as found experimentally by Sun and Chen (1987) for the boron/aluminum composite and by Mignery and Schapery (1988) for the rubber-toughened graphite/epoxy composite; the latter value of c was reported by Lou and Schapery (1971) for glass/epoxy material.

Most of the experimental work reported above is for proportional loading, (17). However, that of Mignery and Schapery (1988) involves nonproportional loading of the plies in an angle-ply layup. These studies provide limited experimental support for (11). We are currently making

additional studies of angle-ply and unidirectional laminates under loading, unloading and reloading to address the applicability of (10) and (42) for toughened and untoughened graphite/epoxy composites.

It should be observed that the difference between loading and unloading curves in the model (6) is characterized by one scalar factor $\partial P/\partial \sigma_o$, where $P = P(\sigma_o, S)$. The loading curves, $d\sigma_o/dt>0$, are predicted by using $S = \sigma_o$. For unloading, $d\sigma_o/dt<0$, the thermodynamic requirement of positive entropy production and the path-independence of the unloading work are violated unless S is constant Schapery (1988). Consequently, for arbitrary stress histories, S is always the largest value of σ_o up to the current time.

This representation does not account for the difference between unloading and reloading curves. Tonda and Schapery (1987) were able to account for this difference for an untoughened graphite/epoxy composites using linear viscoelasticity theory; the approach to combining the effects of viscoelasticity and structure changes was developed earlier (Schapery, 1981). Whether or not this approach is able to account for all of the hysteresis is not presently known. It may be necessary to introduce another S-parameter which is activated at the start of reloading.

3. THE NORMALITY RULE FOR INELASTIC STRAINS

Let us now compare the normality rule employed in plasticity theory to predict plastic strain increments with the type of normality contained in (4). Following Sun and Chen (1987), we take $\sigma_o^2 = k$ as the yield condition, where k is a scalar that varies with the amount of plastic straining. Plastic strains are introduced in the same way as is commonly done for metals,

$$d\varepsilon_i^p = d\varepsilon_i - d\varepsilon_i^e \tag{25}$$

where $d\varepsilon_i^p$, $d\varepsilon_i$, and $d\varepsilon_i^e$ are infinitesmal changes in plastic, total, and elastic strains, respectively. The elastic strains are assumed to be linear in the stresses,

$$\varepsilon_i^e = S_{ij}\sigma_j \tag{26}$$

where S_{ij} are the constant compliances. The associated flow rule for plastic strain increments is

$$d\varepsilon_i^p = \frac{\partial \sigma_o^2}{\partial \sigma_i}\, d\lambda \tag{27}$$

where $d\lambda$ is a scalar. This equation shows that $d\varepsilon_i^p$ is a vector which is normal to the surface σ_o = constant. From (8) and (27),

$$d\varepsilon_i^p = 2a_{ij}\sigma_j d\lambda \tag{28}$$

For proportional stressing $\sigma_i = k_i\sigma_o$ (where the k_i are constants) (28) may be integrated to obtain the total plastic strains,

$$\varepsilon_i^p = \frac{\partial \sigma_o^2}{\partial \sigma_i}(\int \sigma_o d\lambda)/\sigma_o \tag{29}$$

which is also a vector normal to the surface σ_o = constant. The total strain is

$$\varepsilon_i = \varepsilon_i^e + \varepsilon_i^p \tag{30}$$

which may be compared to the strain (6) derived from a dual strain energy density. The "inelastic strain" vector in (6),

$$\varepsilon_i^I \equiv -\frac{\partial P}{\partial \sigma_o}\frac{\partial \sigma_o}{\partial \sigma_i} \tag{31}$$

is normal to the surface σ_o = constant, just as ε_i^P in (29). However, in contrast to ε_i^P, the normality of ε_i^I exists for proportional and non-proportional stressing. Observe also that this normality is preserved during unloading and reloading; recall that the coefficient $\partial P/\partial \sigma_o$ depends on both σ_o and S, and that $S = \sigma_o$ only when σ_o is equal to its largest value (considering all values up to the current time).

Consider next for further comparison a type of normality discussed by Rice (1971) for incremental inelastic strains. He developed (4) from thermodynamics with internal variables and used it in a study of inelastic behavior of metals; S is one of possibly many internal variables. A change in strain due to infinitesimal changes in both σ_i and S is, from (4),

$$d\varepsilon_i = -\frac{\partial^2 w_\sigma}{\partial \sigma_i \partial \sigma_j} d\sigma_j + \frac{\partial G}{\partial \sigma_i} dS \tag{32}$$

where

$$G \equiv -\partial w_\sigma / \partial S \tag{33}$$

Rice observed that when elastic and inelastic strains are defined through increments, as expressed by the first and second terms in (32), respectively, the incremental inelastic strain,

$$d\varepsilon_i^I \equiv \frac{\partial G}{\partial \sigma_i} dS \tag{34}$$

is normal to the"yield" surface G = constant. In fracture mechanics G (33) is called the "energy release rate". When there are two or more structure parameters S_m (m = 1, 2, ...),

$$d\varepsilon_i^I = \frac{\partial G_m}{\partial \sigma_i} dS_m \tag{35}$$

where

$$G_m \equiv -\partial w_\sigma / \partial S_m \tag{36}$$

Thus, the m^{th} component of $d\varepsilon_i^I$ is normal to the respective surface, Sm = constant, as noted by Rice.

When we use the special form for w_σ in (5), Rice's incremental elastic and inelastic strains become

$$d\varepsilon_i^e \equiv -\frac{\partial^2 w_\sigma}{\partial \sigma_i \partial \sigma_j} d\sigma_j = -\frac{\partial^2 w_{\sigma o}}{\partial \sigma_i \partial \sigma_j} d\sigma_j - \frac{\partial^2 p}{\partial \sigma_i \partial \sigma_j} d\sigma_j \tag{37}$$

$$d\varepsilon_i^I \equiv \frac{\partial G}{\partial \sigma_i} dS = -\frac{\partial^2 P}{\partial S \partial \sigma_i} dS = -\frac{\partial^2 P}{\partial S \partial \sigma_o} dS \frac{\partial \sigma_o}{\partial \sigma_i} \tag{38}$$

Notice that $d\varepsilon_i^I$ is normal to the surface σ_o = constant and that an increment in the elastic strain defined in (7) is equal to only the first term in (37). Observe also that the tangent elastic compliance matrix $-\partial w_\sigma / \partial \sigma_i \partial \sigma_j$ used in defining the incremental elastic strains in (32) is a function of the structure parameter S as well as stresses, while that based on the elastic strain in (7), $-\partial^2 w_{\sigma o}/\partial \sigma_i \partial \sigma_j$, depends only on the stresses.

4. A CONSTITUTIVE EQUATION WITH LINEAR UNLOADING BEHAVIOR

In characterizing the effect of damage on composite material behavior, it is commonly assumed that the material is linearly elastic when damage is constant. This linearity assumption is equivalent to using a dual strain energy density in which stress dependence is limited to first and second order terms,

$$w_\sigma = -b_o - b_i\sigma_i - \frac{1}{2} b_{ij}\sigma_i\sigma_j \tag{39}$$

where b_o, b_i and b_{ij} may be functions of one or more structure parameters S_m. In this case the strains (4) are

$$\varepsilon_i = b_i + b_{ij}\sigma_j \tag{40}$$

The residual strains b_i and compliances b_{ij} may vary with stress history through changes in S_m; only one S will be used here. The strain energy density is related to w_σ through (3), and may be written as

$$w = c_o + c_i\,\varepsilon_i + \frac{1}{2} c_{ij}\,\varepsilon_i\,\varepsilon_j \tag{41}$$

which provides the stresses

$$\sigma_i = c_i + c_{ij}\,\varepsilon_j \tag{42}$$

The relationship between the b's and c's may of course be obtained by comparing (40) and (42). These second-order energies may be sufficiently general to predict ply stress-strain behavior if the unloading and reloading curves can be approximated by the same straight line whose position (c_i) and slope (c_{ij}) vary with S (as shown in Fig. 3).

The work ($\int\sigma_i d\varepsilon_i$) and dual work ($-\int\varepsilon_i d\sigma_i$) during structure-change processes are independent of path or history if and only if (Schapery, 1988),

$$-\frac{\partial w_\sigma}{\partial S} = g \quad \text{or} \quad -\frac{\partial w}{\partial S} = g \tag{43}$$

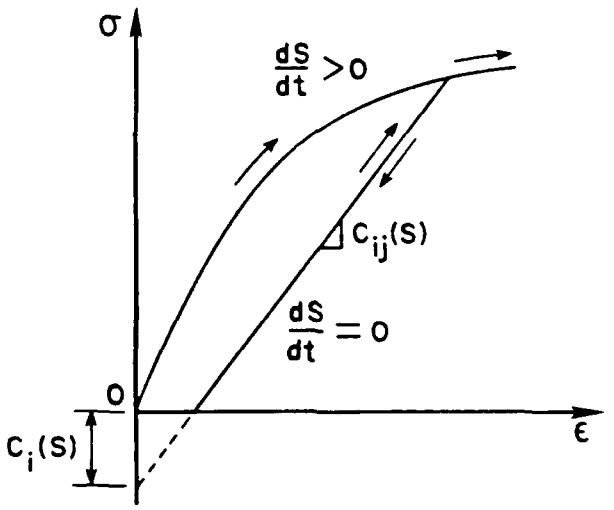

Fig. 3. Stress-strain behavior according to (42), showing loading, unloading and reloading.

where g is at most a function of S; the quantity g is the specific fracture energy if S is the fracture surface area of a crack. (Equation (43) is not limited to the second-order energies (39) and (41).) As shown by Schapery (1988) S can always be chosen so that (43) reduces to

$$-\frac{\partial w_\sigma}{\partial S} = 1 \quad \text{or} \quad -\frac{\partial w}{\partial S} = 1 \tag{44}$$

Observe that the term c_o (= $- b_o$) can be omitted as it can be absorbed in g in (43).

It should be added that the derivatives $\partial w_\sigma/\partial S$ and $\partial w/\partial S$ are always equal which may be easily shown by taking the differential of (3). Equation (44) provides the relationship for predicting S as a function of stress or strain. Thermodynamic theory requires $dS/dt \geq 0$ (Schapery, 1988); thus, if (44) predicts $dS/dt < 0$, S is actually constant and (44) is to be disregarded.

For the second order energy (39) with $b_o = 0$, the equation for S is

$$\frac{db_i}{dS}\sigma_i + \frac{1}{2}\frac{db_{ij}}{dS}\sigma_i\sigma_j = 1 \tag{45}$$

Although (39) is only of second order in the stresses, it is still sufficiently general to mathematically represent Sun and Chen's data discussed in Section 2. Indeed, this may be done by assuming the b_i are constants and then using

$$b_{ij} = S_{ij} + B\,S^r a_{ij} \tag{46a}$$

where

$$r = \frac{n-1}{n+1}, \qquad B = A^{1-r}(2/r)^r \tag{46b}$$

Also, S_{ij} are the constant elastic compliances, and a_{ij}, A, and n are the constants appearing in (8) and (22); observe that $0 \leq r < 1$. Equations (45) and (46) yield

$$S = (Br/2)^{(n+1)/2}\sigma_o^{(n+1)} \tag{47}$$

During loading, $d\sigma_o/dt > 0$, (47) is used in (46a) to predict instantaneous values of b_{ij}. For unloading, $d\sigma_o/dt < 0$, the coefficients b_{ij} are constant because S has a constant value equal to that at the start of unloading. Upon reloading, S again changes in accordance with (47) when σ_o reaches its largest past value. Unloading and reloading data are not reported by Sun and Chen (1987), and thus the range of applicability of this particular model cannot be assessed at this time. It is important to notice that this phenomenological characterization is not necessarily limited to brittle or to ductile composites, as Sun and Chen's results are for both types.

Finally, we should mention that the theory based on path-independence of work has been successfully employed in limited studies of particle-reinforced rubber (Schapery, 1987b), and a thermoplastic composite (Dan Jumbo et al., 1987). In the former case nearly all nonlinear behavior was expressed in terms of S-dependence of b_{ij}; in the latter case the residual strains b_i, instead of b_{ij}, were used to account for most nonlinearities. The small amount of nonlinearity that was not adequately represented by the second-order energy functions was apparently due to the large strains

(≈ 60%) in the filled rubber specimens and fiber or microfibril alignment (causing an increase in modulus for loading in the fiber direction) in the thermoplastic composite.

5. CONCLUDING REMARKS

A possible approach to predicting multidirectional-fiber laminate behavior would consist of using a unidirectional ply energy density, such as given by (5) or (41), with the usual displacement assumptions of lamination theory (Christensen, 1979). Delaminations and their growth could be accounted for essentially in the same way as done for linear and nonlinear elastic laminates, but with additional bookkeeping when there is any appreciable difference between loading and unloading stress-strain behavior. The work of deformation (which is equal to $w_T = w + S$ if the second equation in (44) is used to predict S) is treated just like strain energy in nonlinear elastic fracture mechanics (Schapery,1987a); in particular, w_T is used in strain energy release rate and J integral calculations.

With brittle-matrix composites, a significant number of transverse ply-level cracks may develop prior to structural failure (Johnston, 1987). These cracks are somewhat planar with the plane parallel to the fibers and perpendicular to the lamination plane. Typically, after rapid growth, they are arrested at the ply boundaries. If more than one fiber orientation is used, a laminate usually is capable of supporting loads well above that at crack initiation. Whether or not one S-parameter is sufficient to account for a general type of inelasticity which includes transverse cracks requires further study. It should be observed that even with only one parameter, an appreciable effect of these cracks on the laminate behavior may be taken into account through the way w or w_T depends on S; for example, b_{ij} may have the form in (46a) at small S, and then a considerably different form at large S when transverse cracks develop. Physically, S may reflect micro-damage (e.g. rubber particle cavitation) and plastic deformation until transverse cracks develop, and then at larger S-values account for these mechanisms as well as transverse crack density. If the effects of crack density and its growth are not sensitive to properties of adjacent plies with different fiber angles, an experimental program could use the simple angle-ply layup. Similar observations can be made for distributed interior delaminations (Harris et al., 1987); however, at least two plies would comprise the basic element of a laminate.

We are presently using these ideas to characterize and predict the mechanical response of untoughened and toughened graphite/epoxy laminates, recognizing that the proposed method has to be considered as tentative until a significant amount of additional experimental and analytical studies are made. Such studies should help to establish the range of validity of the work-potential method as well as define the experimental program needed for a complete characterization. Micromechanical models of damage in linear elastic composites (Wang and Haritos, 1987) should be helpful in analytically modeling the effect of distributions of cracks on moduli or compliances, and thus reduce the experimental effort. Schapery (1987b) used this approach in an elementary model to relate the orthotropic elastic properties of a particulate composite to a statistical distribution function which characterized the damage, and employed an evolution equation like (44) to predict the change in properties through an S-parameter which is an overall measure of the damage. A similar procedure should be applicable to laminates.

ACKNOWLEDGEMENT

The author is grateful to the U.S. Air Force Office of Scientific Research for sponsoring this research.

REFERENCES

Christensen, R.M. (1979). Mechanics of Composite Materials, John Wiley & Sons, New York.

Dan Jumbo, E.A., B.C. Harbert, and R.A. Schapery (1988). Constant rate, creep behavior, and the analysis of thermoplastic composite laminates. Presented at the ASTM 9th Symposium on Composite Materials: Testing and Design.

Harris, C.E., D.H. Allen and E.W. Nottorf (1987). Damage-induced changes in the Poisson's ratio of cross-ply laminates: an application of a continuum damage mechanics model for laminated composites. In: Damage Mechanics in Composites (A.S.D. Wang and G.K. Haritos, eds.), AD-Vol. 12, pp. 17-23. American Society of Mechanical Engineers, New York.

Johnston, N.J. (1987). Toughened Composites, STP 937, American Society for Testing and Materials (ASTM), Philadelphia.

Lamborn, M.J. and R.A. Schapery (1988). An investigation of deformation path-independence of mechanical work in fiber-reinforced plastics. In: Proc. 4th Japan-U.S. Conference on Composite Materials, Technomic.

Lou, Y.C. and R.A. Schapery (1971). Viscoelastic characterization of a nonlinear fiber-reinforced plastic. J. Composite Materials, 5, 208-234.

Mignery, L. and R.A. Schapery (1988). Effect of adherend inelasticity on bonded composite joints. Texas A&M Univ. Report No. 5558-88-14.

Rice, J.R. (1971). Inelastic constitutive relations for solids: an internal-variable theory and its application to metal plasticity. J. Mechanics and Physics of Solids, 19, 433-455.

Schapery, R.A. (1981). On viscoelastic deformation and failure behavior of composite materials with distributed flaws. In: 1981 Advances in Aerospace Structures and Materials (S.S. Wang and W.J. Renton, eds.). The American Society of Mechanical Engineers, New York, 5-20.

Schapery, R.A. (1987a). Deformation and fracture characterization of inelastic composite materials using potentials. Polymer Engineering and Science, 27, 63-76.

Schapery, R.A. (1987b). Nonlinear constitutive equations for solid propellant based on a work potential and micromechanical model, Proc. 1987 JANNAF Structures and Mechanical Behavior Meeting, (Texas A&M Univ. Report No. MM-5488-87-4).

Schapery, R.A. (1988). A theory of mechanical behavior of elastic media with growing damage and other changes in structure. Texas A&M Univ. Report No. MM 5762-88-1.

Sun, C.T. and J.L. Chen (1987). A simple flow rule for characterizing nonlinear behavior of fiber composites. In: Proc. Sixth Int. Conf. on Composite Materials (F.L. Matthews, N.C.R. Buskell, J.M. Hodgkinson, J. Morton, eds.), Elsevier, London, pp. 1.250-259.

Tonda, R.D. and R.A. Schapery (1987). A method for studying composites with changing damage by correcting for the effects of matrix viscoelasticity. In: Damage Mechanics in Composites (A.S.D. Wang and G.K. Haritos, eds.), AD-Vol. 12, American Society of Mechanical Engineers, New York, pp. 45-51.

Wang, A.S.D. and G.K. Haritos (1987). Damage Mechanics in Composites, AD-Vol. 12, American Society of Mechanical Engineers, New York.

Yee, F. (1987). Modifying matrix materials for tougher composites. In: Toughened Composites (N. Johnston, ed.), STP 937, pp. 383-396. ASTM, Philadelphia.

Report No. MM 5762-89-10
April 1989

MECHANICAL CHARACTERIZATION AND ANALYSIS OF INELASTIC COMPOSITE LAMINATES WITH GROWING DAMAGE*

R.A. Schapery

Civil Engineering Department

Texas A&M University

College Station, TX 77843

ABSTRACT

A method of laminate characterization and analysis is described in which growing damage and other inelastic phenomena are treated using the same mathematical formalism, thus simplifying the description of mechanical response. It is based on the observation that the applied work is not sensitive to many details of the deformation history. Following a brief discussion of the thermodynamically-based theory, we use a special version along with experimental data on a graphite/epoxy composite to obtain an explicit mathematical characterization of a unidirectional ply. Predictions of mechanical response are then compared to experimental results for a variety of layups, one of which delaminates from the edges.

NOMENCLATURE

a	Delamination depth
b, c, r	Coefficients in strain energy
E_x, E_1, E_2	Young's Modulus GPa ($lb/in^2 x10^6$)
f_m	Thermodynamic force
f_1, f_2, f_{12}	Strain-dependent coefficients
G_{12}	Shear modulus GPa ($lb/in^2 x10^6$)
Q_{ij}	Reduced modulus
S, S_i, S_m	Structural parameter
S, w_s	Work needed for structural changes/vol
S_R	Cube root of S
w, w_o	Strain energy/vol
w_T	Total work input/vol
W_T	Total work input
x_k	Cartesian coordinate
ϵ, ϵ_i	Strain
ν, ν_{12}, N_x	Poisson's ratio
σ, σ_i	Stress ($lb/in^2 x10^3$)

1. INTRODUCTION

The nonlinear behavior of unidirectional and multidirectional fiber composites traditionally has been modeled using elasticity theory (1) or plasticity theory in which the unloading moduli are constant (2,3). However, resin matrix composites often exhibit nonlinear behavior which is due at least in part to inelastic mechanisms that alter the unloading moduli. As illustrated in Fig. 1 for

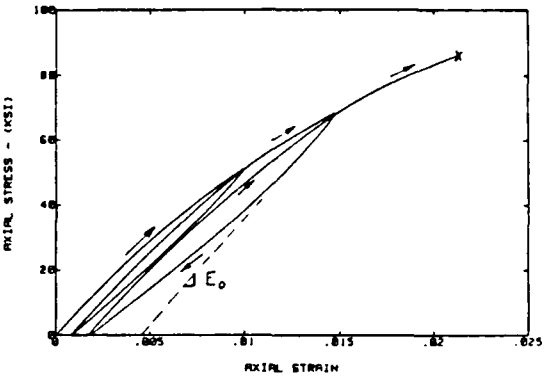

Fig. 1 Stress-strain behavior of Hercules AS4/3502 angle-ply laminate $[\pm 30]_{3S}$ showing inelastic behavior.

the brittle-resin composite studied later in this paper, the inelasticity (i.e. strain history-dependence) is neither small enough to neglect nor large enough to use classical plasticity theories in which unloading follows the initial modulus E_o. For several unidirectional and angle-ply layups of this graphite/epoxy material we have found that the residual strain upon load removal is typically 20-40% of that for unloading along the E_o-line. There is also a small amount of rate or time-dependence even in the room environment.

In this paper we discuss a way of characterizing nonlinear inelastic behavior that may arise from a variety of mechanisms, including microcracking, delamination, void growth, shear yielding, and crystalline slip, and therefore is not limited to resin-matrix or metal-matrix composites. It is based on the theory in (4), which uses Rice's (5) thermodynamic description of inelastic behavior. Some motivation for the theory has come from our experimental studies of rubber-toughened and untoughened graphite/epoxy (6,7) under axial-torsional loading, which show that the stresses and mechanical work are practically independent of deformation history for suitably limited paths. This limited path-independence leads to a mathematical description of mechanical behavior which is analogous to that used for predicting stable crack growth and its effect on global structural response.

In Section 2 the theory for a unidirectional ply or laminate is outlined, and the plane-stress case used in later sections is described; the theory allows for elastic nonlinearity (such as that due to fiber-straightening) and inelastic nonlinearity during loading. Sections 3-5 discuss the experimental program and both linear and nonlinear behavior; after the basic ply characterization is accomplished, response of several laminates is predicted and shown to be in good agreement with the experimental findings.

*Published in Mechanics of Composite Materials and Structures, ASME AMD-Vol. 100, 1-9, 1989.

2. CONSTITUTIVE EQUATIONS FOR A UNIDIRECTIONAL PLY

Basic theory

The coordinate notation for a unidirectional laminate or ply is shown in Fig. 2; the x_1 axis is parallel to the fibers while the x_3 axis is normal to the ply plane. The stresses σ_j and strains

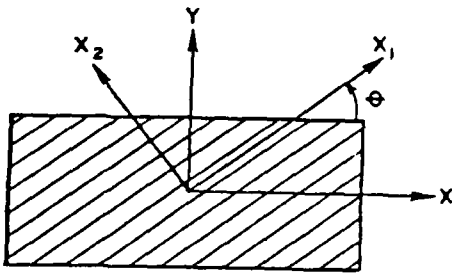

Fig. 2 Unidirectional composite and coordinates

ε_j (i=1,2,...6) are referred to the principal material coordinates x_k(k=1,2,3). We also employ the standard notation in which i=4,5,6 refer to the shearing stresses and strains, where these shearing strains are twice the tensor components.

The stresses are related to strains through the strain energy density (per unit initial volume) $w = w(\varepsilon_i, S_m)$,

$$\sigma_i = \partial w/\partial \varepsilon_i \qquad (1)$$

where the S_m are so-called "structural parameters". Temperature and other parameters (such as moisture) may enter; but for simplicity we assume they are constant, and thus do not explicitly show them as arguments. As many S_m as needed are used to account for the microstructural changes which produce the inelastic behavior.

It will be helpful to also use the dual strain energy density $w_o = w_o(\sigma_i, S_m)$,

$$w_o \equiv w - \sigma_i \varepsilon_i \qquad (2)$$

which is seen to be the negative of the complementary strain energy density. The summation convention is employed wherein a repeated index implies summation over its range. By using Eq. (1) with the differential of Eq. (2) for constant S_m, we find

$$\varepsilon_i = -\partial w_o/\partial \sigma_i \qquad (3)$$

Changes in S_m may be related to stresses or strains by using a constitutive equation for the thermodynamic forces f_m; these forces are, by definition,

$$f_m \equiv -\partial w/\partial S_m \qquad (4)$$

The differential of Eq. (2), for independent changes dS_m, yields

$$f_m = -\partial w_o/\partial S_m \qquad (5)$$

The second law of thermodynamics allows only those changes for which

$$f_m \dot{S}_m \geq 0 \qquad (6)$$

where the overdot denotes a derivative with respect to time. As the constitutive equation for f_m, we specify that for each active parameter, i.e. $\dot{S}_m \neq 0$,

$$f_m = \partial w_s/\partial S_m \qquad (7)$$

where $w_s = w_s(S_m)$ is a constitutive function of S_m; also, for those m in which $f_m \neq \partial w_s/\partial S_m$ then $\dot{S}_m = 0$. Each f_m is viewed as the force available to produce changes in the associated S_m, while $\partial w_s/\partial S_m$ is the force required for these changes. The solution of Eq. (7) yields $S_m = S_m(\varepsilon_i)$ or $S_m = S_m(\sigma_i)$ for each active parameter.

The total work input per unit initial volume during actual elastic or inelastic processes is

$$w_T = \int_0^{\varepsilon} \sigma_i d\varepsilon_i \qquad (8)$$

It is always possible to select ε_i and S_m such that they vanish in the initial or reference state, and therefore we use such a choice throughout this paper. Given Eq. (7), one may easily show that w_T is a potential function of the state (ε_i, S_m) and, in particular, that

$$w_T = w + w_s, \quad \sigma_i = \partial w_T(\varepsilon_j, S_m(\varepsilon_j))/\partial \varepsilon_i \qquad (9)$$

(Without loss in generality we specify that $w = w_s = 0$ in the initial state.) According to Eq. (9), the total work consists of the work of straining w plus the work of structural change w_s. Moreover, from Eqs.(6) and (7),

$$\dot{w}_s \geq 0 \qquad (10)$$

Quadratic strain energy functions

Consider now as a candidate dual strain energy the quadratic form

$$w_o = -b_o - b_i\sigma_i - \frac{1}{2} b_{ij}\sigma_i\sigma_j + \frac{1}{2} r_{ij}(S_i - \sigma_i)(S_j - \sigma_j) \qquad (11)$$

The last term allows for up to six independent structural parameters, while all coefficients may depend on these as well as other parameters; unless this dependency is restricted in some way the last term is redundant. The strain Eq. (3) becomes

$$\varepsilon_i = b_i + b_{ij}\sigma_j + r_{ij}(S_j - \sigma_j) \qquad (12)$$

Both b_i and r_{ij} contribute to the residual strains (i.e. the strains when $\sigma_i \equiv 0$). As a further specialization of the theory, we assume that the b_i are independent of S_m and S_i and that the remaining coefficients b_{ij} and r_{ij} depend on only one parameter, S, which we take to be w_s. The term b_o affects only Eq. (7), and can be absorbed into w_s, although the inequality (10) would still apply only to w_s. When the S_m define only the state of damage in the form of cracks and voids, b_o is the surface free energy, and thus may be viewed as the energy available for healing; here we assume $b_o \equiv 0$ so that $\dot{S} \geq 0$.

With these restrictions on the coefficients, Eqs. (5) and (7) yield

$$\frac{\partial w_o}{\partial S} = -1 \quad \text{if} \quad \dot{S} \neq 0 \qquad (13)$$

and

$$r_{ij}(S_j - \sigma_j) = 0 \quad \text{if} \quad \dot{S}_i \neq 0 \qquad (14)$$

If all $\dot{S}_i \neq 0$ and if r_{ij} is positive definite, then Eq.

(14) implies

$$S_j = \sigma_j \tag{15}$$

and Eq. (12) reduces to

$$\epsilon_i = b_i + b_{ij}\sigma_j \tag{16}$$

while Eq. (13) becomes

$$\frac{1}{2}\frac{db_{ij}}{dS}\sigma_i\sigma_j = 1 \tag{17}$$

We may now give a physical interpretation for the three sets of coefficients in Eqs.(11) and (12). The b_{ij} are compliances that in general vary with the work done in changing the microstructure, S. Since $S = w_s$, Eq. (10) implies $\dot{S} \geq 0$. If we know the functions $b_{ij}(S)$, then Eq. (17) may be used to predict S in terms of stress history; if the equation predicts $\dot{S} < 0$, then we set $S = S_\ell$, where S_ℓ is the largest value of S up to the current time. If Eq. (17) is subsequently satisfied, then again it is used to predict S.

Whenever $S_j \neq \sigma_j$, then instead of Eq. (16) we have from Eq. (12),

$$\epsilon_i = b_i + r_{ij}S_j + (b_{ij} - r_{ij})\sigma_j \tag{18}$$

It is seen that by means of r_{ij} we may simulate the effect of internal surface roughness and other irregularities in resisting crack closing and sliding and void collapse during unloading; whenever all $S_j = \sigma_j$ these coefficients have no effect on the strain, Eq. (16). Had we allowed for dependence of b_i on S_m, then these coefficients would produce the type of residual strains usually associated with plastic deformation mechanisms, such as crystalline slip.

The strain energy density w corresponding to Eq. (11) may be obtained from Eq. (2) after stresses are expressed in terms of strains. Whether or not the r_{ij} enter, it is of the form

$$w = c_o + c_i\epsilon_i + \frac{1}{2}c_{ij}\epsilon_i\epsilon_j \tag{19}$$

From Eq. (1),

$$\sigma_i = c_i + c_{ij}\epsilon_j \tag{20}$$

By comparing Eq. (20) to (16) or (18), we may obtain the coefficients in Eq. (20) in terms of those in the former equations. Figure 3 illustrates the loading

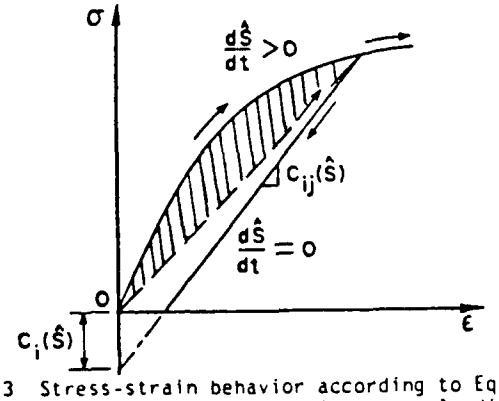

Fig. 3 Stress-strain behavior according to Eq. (20), showing loading, unloading and reloading.

and unloading behavior in terms of the coefficients in Eq. (20), where $\hat{S}$ represents all structural parameters.

In all of the subsequent work we shall be concerned with only loading processes, defined here as those for which $\dot{S} > 0$ as well as $S_j = \sigma_j$ or else $r_{ij} = 0$. Moreover, we shall assume $b_i = c_i = 0$, except in a brief discussion on thermal residual strains. With these simplifications

$$w = \frac{1}{2}c_{ij}\epsilon_i\epsilon_j \tag{21}$$

and

$$\sigma_i = c_{ij}\epsilon_j \tag{22}$$

Also noting that Eqs. (4) and (5) imply $\partial w/\partial S = \partial w_o/\partial S$, then from Eq. (13),

$$\frac{\partial w}{\partial S} = -1 \tag{23}$$

From Eq. (9)

$$S = w_T - w \tag{24}$$

which shows that the instantaneous value of S is the shaded area in Fig. 3.

Constitutive equations for plane stress

Constitutive Eq. (22) has the same form as that for a linear elastic material. If we assume the material is orthotropic, with principal material directions x_k, then we may use standard linear elastic equations to characterize ply behavior in terms of principal moduli. From (8),

$$\sigma_1 = Q_{11}\epsilon_1 + Q_{12}\epsilon_2 \tag{25a}$$

$$\sigma_2 = Q_{12}\epsilon_1 + Q_{22}\epsilon_2 \tag{25b}$$

$$\tau_{12} = Q_{66}\gamma_{12} \tag{25c}$$

where

$$Q_{11} = E_1/D \ , \quad Q_{22} = E_2/D \tag{26a}$$

$$Q_{12} = \nu_{12}Q_{22} \ , \quad D = 1 - \nu_{12}\nu_{21} \tag{26b}$$

$$\nu_{21} = \nu_{12}E_2/E_1 \ , \quad Q_{66} = G_{12} \tag{26c}$$

Only the Young's modulus for loading normal to the fibers E_2 and the shear modulus G_{12} are assumed to vary as a result of inelastic mechanisms. The remaining two principal properties, i.e. Young's modulus in the fiber direction E_1 and Poisson's ratio ν_{12}, are assumed to be independent of S, which is reasonable if the fibers do not break. Indeed, our experimental results from loading and unloading tests parallel to the fibers show negligible hysteresis in axial and transverse strains, even when the maximum strain is close to the ultimate value. However, there is some elastic nonlinearity which is not negligible for our purposes; E_1 increases and E_2 and ν_{12} decrease with increasing strain.

In order to account simultaneously for inelastic effects in E_2 and G_{12} and nonlinear elastic effects in E_1, E_2 and ν_{12} we propose the following modified form of Eq. (25),

$$\sigma_1 = Q_{11}f_1\epsilon_1 + \nu Q_{22}f_{12}I_2 \tag{27a}$$

$$\sigma_2 = \nu Q_{22}f_2I_1 + Q_{22}f_2\epsilon_2 \tag{27b}$$

$$\tau_{12} = G_{12}\gamma_{12} \tag{27c}$$

where

$$\nu \equiv \nu_{12}(o),\ I_1 \equiv \int_o^{\varepsilon_1} f_{12}d\varepsilon_1\ ,\ I_2 = \int_o^{\varepsilon_2} f_2 d\varepsilon_2 \tag{28}$$

and

$$f_1 \equiv \frac{E_o(\varepsilon_1)}{E_1(0)}\ ,\quad f_{12} = -\frac{1}{\nu}\frac{d\varepsilon_2}{d\varepsilon_1}\ ,\quad f_2 \equiv \frac{E_{90}(\varepsilon_2)}{E_2(0)} \tag{29}$$

The strain-dependent functions f_1 and f_{12} are the ratios of the secant modulus $E_o = \sigma_1/\varepsilon_1$ and tangent Poisson's ratio at a given axial strain to those at $S = \varepsilon_1 = 0$ (for $\sigma_1 \neq 0$, $\sigma_2 = \tau_{12} = 0$). Allowance has been made for elastic nonlinearity under transverse loading ($\sigma_2 \neq 0$, $\sigma_1 = \tau_{12} = 0$) through f_2; the quantity E_{90} in Eq. (29) is the secant modulus for S = 0 from the 90° specimen. Observe that $I_1 = -\varepsilon_2(\varepsilon_1)/\nu$, where this ε_2 is the transverse strain in a uniaxial test with $\sigma_1 \neq 0$, $\sigma_2 = \tau_{12} = 0$.

The factor D in Eq. (26b) is practically unity, and although it is not constant we may use its initial linear elastic value in all work without any significant error. All strain dependence of the moduli is now accounted for through f_1, f_2, and f_{12}, and therefore Q_{11} and Q_{22} in Eq. (27) are those in Eq. (26a); viz., E_1 and Q_{11} are constants, while Q_{22} varies with S through E_2; E_2 and G_{12} now vary only with S.

The form of Eq. (27a) and Eq. (27b) is such that

$$\frac{\partial\sigma_1}{\partial\varepsilon_2} = \frac{\partial\sigma_2}{\partial\varepsilon_1} \tag{30}$$

which is a necessary and sufficient condition for construction of the strain energy function in Eq. (1). We find that

$$w = Q_{11}I_{11} + Q_{22}I_{22} + \nu Q_{22}I_2I_1 + G_{12}\gamma_{12}^2/2 \tag{31}$$

where

$$I_{11} = \int_o^{\varepsilon_1} \varepsilon_1 f_1 d\varepsilon_1\ ,\quad I_{22} \equiv \int_o^{\varepsilon_2} \varepsilon_2 f_2 d\varepsilon_2 \tag{32}$$

When the elastic behavior is linear Eq. (31) reduces to

$$w = (Q_{11}\varepsilon_1^2 + Q_{22}\varepsilon_2^2 + 2\nu Q_{22}\varepsilon_1\varepsilon_2 + G_{12}\gamma_{12}^2)/2 \tag{33}$$

An alternative characterization in terms of stresses using the dual energy was also developed. For linear elastic behavior it is equivalent to the strain formulation. The elastic nonlinearity was not introduced by using Eq. (31) in Eq. (2); instead, for simplicity w was constructed to be similar in form to Eq. (31), but with stress-dependent functions as found from the uniaxial stress tests. All predictions made with this stress formulation were virtually the same as found from the strain formulation, Eq. (31). As the strain formulation is far more convenient for predicting response of multi-directional fiber laminates, we use only this formulation here.

3. EXPERIMENTAL PROGRAM

The composite material used in all experimental work was a graphite fiber-reinforced epoxy, Hercules' AS4/3502 with a 64.2% fiber volume fraction. It was supplied in unidirectional prepreg form and cured in our air-cavity press using the supplier's specification for the cure cycle. The specimens were cut from 12"x12" plates and stored in a dessicant until they were strain-gaged and tested under uniaxial loading in an ambient environment of about 75°F and at a tensile strain rate of 0.005/min.

All unidirectional and angle-ply layups consisted of 12 plies. Most specimens were 0.5 inch wide, with a length of 7.5 inches between the glass-epoxy end-tabs. Some 1x10 inch specimens were also tested for comparison purposes; no significant differences between the 0.5 and 1.0 inch wide specimens were found. By screening out all samples whose thicknesses differed by more than 5%, very little specimen-to-specimen differences in mechanical behavior were observed. In most cases the results presented are for an average of two specimens. The off-axis, unidirectional specimens exhibited the greatest variability, but we have not attempted to quantify the scatter. Two pairs of axial and transverse foil strain gages were used on front and back surfaces in order to average out any through-thickness bending. All readings were corrected for gage transverse sensitivity and strain nonlinearity using the manufacturer's data. Several specimens were tested using two cycles of tensile loading, unloading, and reloading at successively higher maximum strains.

The specific layups used for the chracterization phase and the theoretical-experimental comparisons are identified in subsequent sections.

4. LINEAR ELASTIC BEHAVIOR

Elastic constants

The principal properties are

$$E_1 = 125.5(18.2),\ \nu = 0.334,$$
$$E_2 = 9.38(1.36),\ G_{12} = 5.22(0.757) \tag{34}$$

where the moduli are in GPa(Msi). Chebyschev polynomials were fit to all stress-strain curves and the first-order coefficients provided the results in Eq. (34). Unidirectional 0° and 90° layups provided (E_1, ν) and E_2, respectively, while the angle-ply laminate $[\pm 45]_{3S}$ provided G_{12} from

$$G_{12} = E_x/2(1+N_x) \tag{35}$$

where E_x and N_x are the Young's modulus and Poisson's ratio of the laminate; although this equation is the same as for an isotropic material, it really comes from lamination theory.

Predictions for unidirectional and angle-ply laminates

Predictions based on Eq. (34) and standard linear theory are shown by the continuous lines in Figs. 4 and 5.

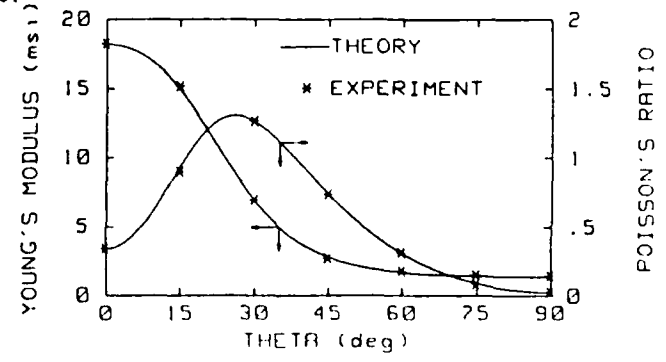

Fig. 4 Modulus and Poisson's ratio of the angle-ply laminate versus fiber angle

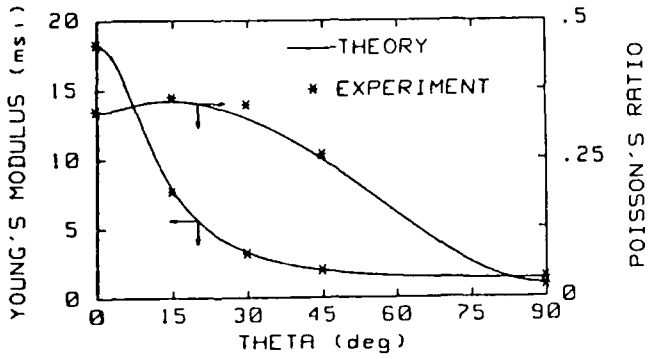

Fig. 5 Modulus and Poisson's ratio of the unidirectional laminate versus fiber angle

Agreement between theory and experiment is excellent except for the off-axis unidirectional Poisson's ratio.

Sensitivity study

The very low failure strain of the 90° specimen precludes its use for determining E_2 as a function of S. In order to identify good layups for finding E_2 as well as G_{12}, the sensitivity of Young's modulus E_x and Poisson's ratio N_x to E_2 and G_{12} was calculated. Figures 6 and 7 show the results for angle-ply

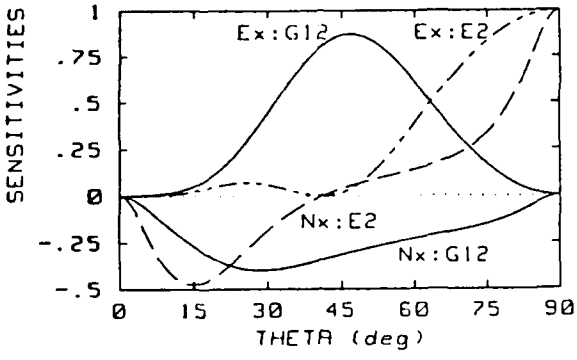

Fig. 6 Effect of changes in G_{12} and E_2 on Young's modulus E_x and Poisson's ratio N_x for the angle-ply laminate

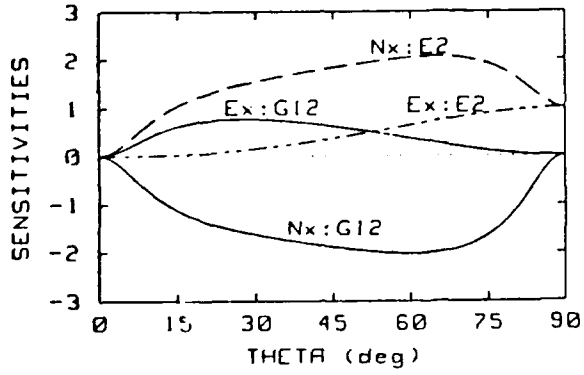

Fig. 7 Effect of changes in G_{12} and E_2 on Young's modulus E_x and Poisson's ratio N_x for the unidirectional laminate

(±θ) and unidirectional (θ) laminates, where θ is the angle between the loading and fiber directions. The sensitivitites are logarithmic derivatives; for example $E_x:E_2$ is the plot of

$$\frac{a\log E_x}{a\log E_2} = \frac{E_2}{E_x}\frac{aE_x}{aE_2} \qquad (36)$$

Thus, an ordinate value of 0.75 implies a 1% change in E_2 produces a 0.75% change in E_x. The modulus and Poisson's ratio of the (±45°) layup are practically independent of E_2, and therefore some other layup is needed to obtain E_2. Although the sensitivity to E_2 is good at large angles, the failure strain is quite low. The (±30°) layup provides adequate sensitivity and a relatively high failure strain, and therefore it was selected to obtain E_2. Sensitivities in Fig. 7 are quite good for most unidirectional layups. The high failure strain we found for the 15° layup seems to make this a good choice; however, as discussed later, there appears to be some difference between the intrinsic nonlinear behavior of unidirectional and angle-ply laminates.

5. NONLINEAR BEHAVIOR

Material characterization

Figures 8 and 9 show the experimental mechanical

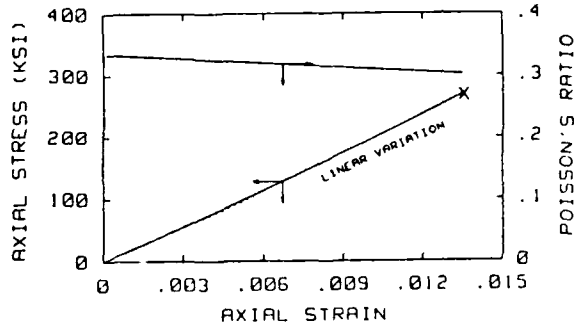

Fig. 8 Behavior of $|0|_{12}$ laminate

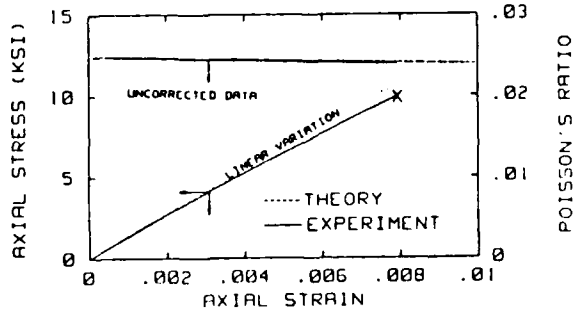

Fig. 9 Behavior of $|90|_{12}$ laminate

behavior (out to the ultimate strain) for the 0° and 90° specimens, respectively. Both modulus and Poisson's ratio are seen to vary somewhat with strain. Data from load-unload-reload tests showed negligible departures from the single-load 0° curves, as noted previously. Roughly 75% of the nonlinear behavior in the 90° curve was retraced, and thus we used for $E_{90}(\epsilon_2)$ in Eq. (29) a secant modulus with 25% less nonlinearity than found directly from the 90° test data. Second order Chebyschev polynomials were found to represent the 0° and 90° data very accurately; the uncorrected data for Poisson's ratio in Fig. 9 were adjusted by a constant factor so that the initial value of ν_{21} agreed with the first expression in Eq. (26c); apparently, the manufacturer's transverse sensitivity correction factor for the transverse strain gage is not sufficient to fully account for this sensitivity when the Poisson's ratio is very small. The polynomials were used to evaluate the secant moduli and tangent Poisson's ratio in Eq. (29). The top dashed line in Fig. 9 is the predicted Poisson's ratio from Eq. (27) when all nonlinearity is elastic.

In order to complete the characterization needed for Eq. (27), $E_2 = E_2(S)$ and $G_{12} = G_{12}(S)$ were obtained from the (±30°) and (±45°) data in Figs. 10 and 11.

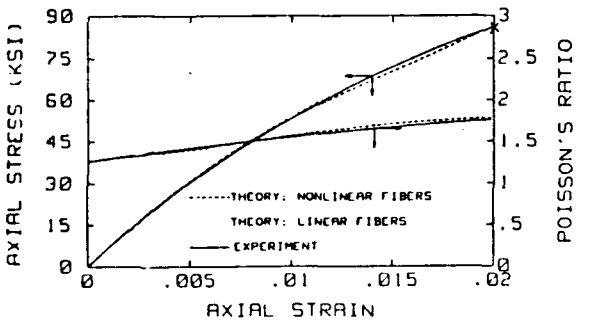

Fig. 10 Behavior of $[\pm 30]_{3S}$ laminate

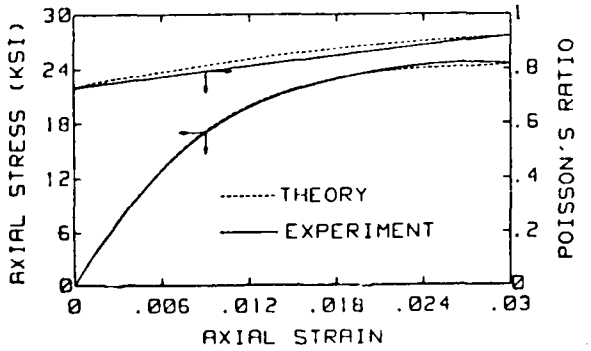

Fig. 11 Behavior of $[\pm 45]_{3S}$ laminate

In Eq. (27), $Q_{11} = E_1(o)/D$ and $Q_{22} = E_2(S)/D$, where, as an excellent approximation, we have used the linear elastic constants from Eq. (34) to find $D = 0.992$.

After completing the characterization, we predicted the inelastic behavior (S>0) of the (±45) specimen using the linear elastic ($f_1 = f_2 = f_{12} = 1$) and nonlinear elastic representations. No significant difference was found. Consequently, one may use Eq. (35) to obtain G_{12} from the data in Fig. 11.

To find E_2, Eq. (27) was rewritten in terms of specimen coordinates (x,y) using second order tensor transformations for the stresses and strains. Then, by using the condition that $\gamma_{xy} = 0$ for an angle-ply laminate, the axial modulus E_x and Poisson's ratio N_x were expressed as functions of G_{12} and E_2. This result enabled us to find G_{12} and E_2 as a function of the axial strain. Although the (±30°) specimen provides both G_{12} and E_2, we found that the higher ultimate strain of the (±45°) specimen enabled G_{12} to be determined out to a 17% larger value of S, and thus only the latter G_{12} was used subsequently. The modulus E_2 was predicted out to the same maximum S using the polynomial.

The procedure discussed thus far provides E_2 and G_{12} as a function of axial strain from each of the specimens. It remains to relate these strains to the structure-change work S, as given by Eq. (24). When the elastic nonlinearity is neglected, then $w = \sigma_x \epsilon_x/2$, so that this work for unidirectional and angle-ply laminates at any given axial strain ϵ_x is the shaded area illustrated in Fig. 3. With elastic nonlinearity then Eq. (31), expressed in specimen coordinates, provides w. In the neighborhood of the initial state ($\epsilon_x = S = 0$), both w_T and w vary as ϵ_x^2, and their difference, S, varies as ϵ_x^3. Moreover, both G_{12} and E_2 have non-zero first order coefficients in ϵ_x. Therefore, in order to fit G_{12} and E_2 with Chebyschev polynomials, $S_R = S^{1/3}$, rather than S, was used as the expansion parameter.

The continuous lines in Fig. 12 for G_{12} and E_2 were

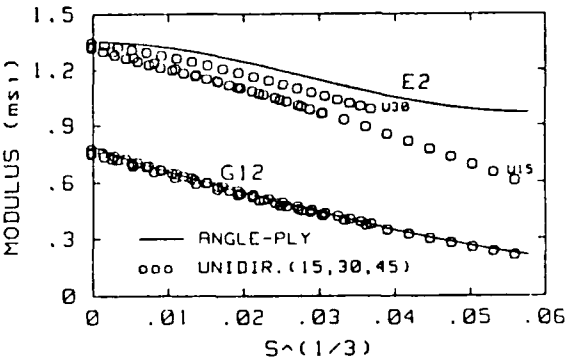

Fig. 12 Transverse and shear moduli versus cube root of the structure-change work

plotted using a sixth-order polynomial fit in S_R to the data from (±45°) and (±30°) specimens; the units used for S are Msi. The data points show moduli found from 15°, 30°, and 45° unidirectional specimens, neglecting the elastic nonlinearity. The effect of this nonlinearity was estimated as being too small to account for the differences shown for E_2.

Predictions

All material functions (f_1, f_2, f_{12}) and (G_{12}, E_2) have been expressed as polynomials in strain and S_R.

respectively. In order to predict the instantaneous value of S in each ply of a laminate we may use (23). This expression is a nonlinear algebraic equation for S, given the strains. The strain energy function is in Eq. (31) or (33). Prediction of ply strains, for each S, was done using lamination theory (8). The numerical method employed consisted of solving simultaneously for the unknown ply strains and S, given the axial strain, using the Newton-Raphson method; usually only a few iterations (2 to 5) were needed for convergence to a relative error of 10^{-4}. We should add that since S_R was used as the polynomial expansion parameter, we changed Eq. (23) to the form

$$\frac{1}{S_R}\left(\frac{\partial w}{\partial S_R} + 3S_R^2\right) = 0 \qquad (37)$$

and then used the Newton-Raphson method to drive the left side to zero; the indicated division by S_R increased the rate of convergence.

All predictions that follow are based on the G_{12} and E_2 in Fig. 12 found from the angle-ply specimens; the nonlinear elastic behavior was accounted for. When both G_{12} and E_2 were found from the (±30°) data in Fig. 10, differences between theory and experiment in Fig. 10 could not be discerned whether nonlinear elasticity ("nonlinear fibers") or linear elasticity ("linear fibers") was used, as expected. However, for the results reported here only one function was used from each of the two laminates. Thus, the predictions in Figs. 10 and 11 provide a partial check on the theory.

Figures 13-19 show additional predictions

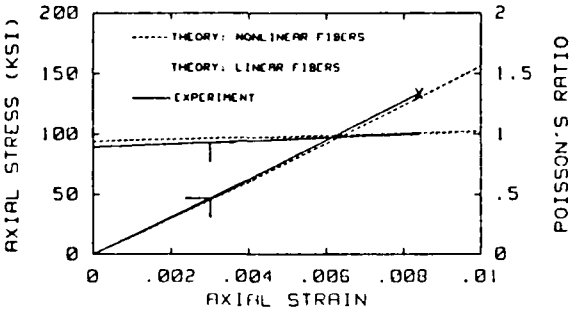

Fig. 13 Behavior of $[\pm 15]_{3S}$ laminate

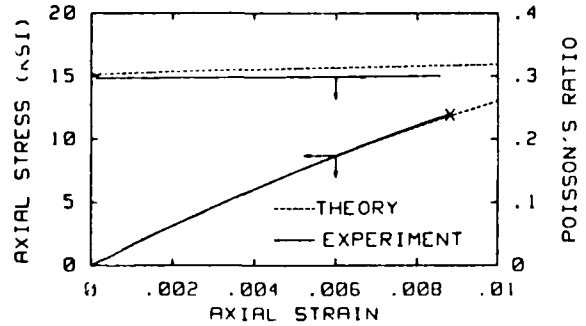

Fig. 14 Behavior of $[\pm 60]_{3S}$ laminate

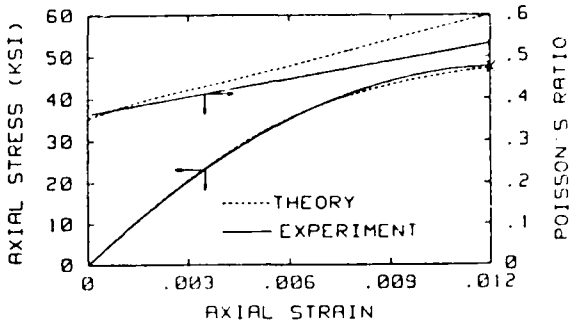

Fig. 15 Behavior of $[15]_{12}$ laminate

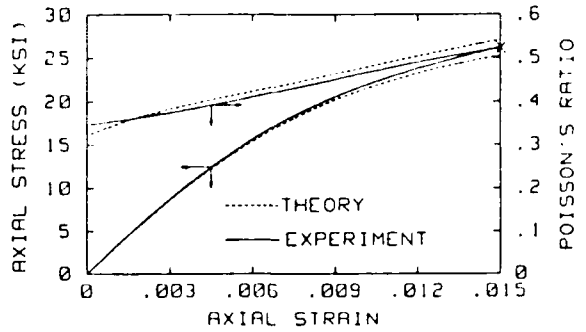

Fig. 16 Behavior of $[30]_{12}$ laminate

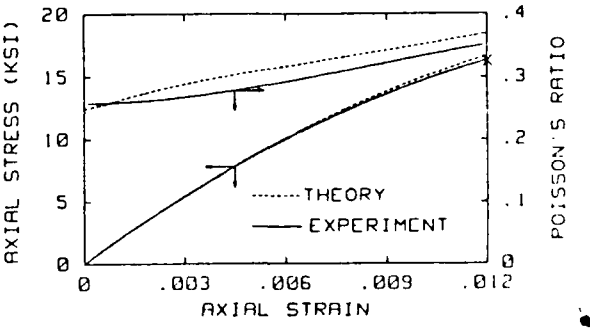

Fig. 17 Behavior of $[45]_{12}$ laminate

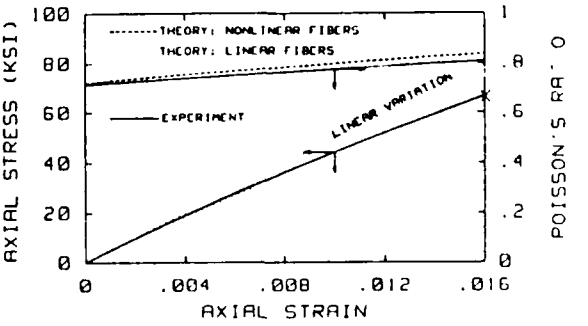

Fig. 18 Behavior of $[+45/-45/+45/45/0/+45/-45]_S$ laminate.

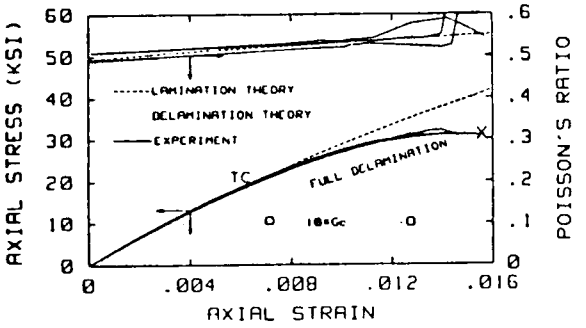

Fig. 19 Behavior of $[+45/-45/+45/-45/90/+45/-45]_S$ laminate

for angle-ply, unidirectional, and tridirectional laminates. In most cases there was little difference between the nonlinear fiber and linear fiber ($f_1 = f_2 = f_{12} = 1$) predictions, and so only the nonlinear case is shown. Inclusion of the elastic nonlinearity always improved the prediction. The "linear variation" in Fig. 18 uses the initial modulus; it emphasizes the softening effect of S in the 45° plies. The axial stress prediction using nonlinear fibers is essentially the same as the measured stress.

Figure 19 shows results from three replicate tests of a laminate that was selected for its susceptibility to edge delamination. Indeed, delamination was observed to gradually develop at the edge and then grow inward, beginning at a strain of about 0.008. Full delamination and specimen failure occurred at approximately twice this strain. Transverse cracking (TC) in the 90° plies initiated just before edge delaminations were observed. The Poisson's ratio was not affected by the delamination until it reached the centrally located strain gages.

For the laminate in Fig. 18 the 0° plies are under a compressive transverse stress, while the 90° plies for that in Fig. 19 have a compressive stress parallel to their fibers. In both cases, this compression is due to the relatively high Poisson's ratio of the (±45) ply-pair (cf. Fig. 11). No adjustment was made to the nonlinear elastic coefficients f_1, f_2, and f_{12} to account for this compression, even though they were determined under tensile loading; as these coefficients turned out to be linear in strain, a stiffening nonlinearity in tension becomes a softening nonlinearity in compression and vice-versa. When elastic nonlinearity was neglected, the agreement with experimental data was not quite as good as when it was used.

Delamination analysis

Prediction of the delamination in the laminate of Fig. 19 may be accomplished using the same method as for an elastic material, except the work potential density w_T replaces strain energy density w (4,6). The two lowest dotted curves in Fig. 19 are strain energy release rates x 10 (referred to the left axis) for an edge delamination in the outer interface between the -45 and 90 plies. They were found by adapting O'Brien's method (9) to the present formulation, as noted above. Basically, one first adds the work potential density $w_T^{(1)}$ of the central, undelaminated section to those of the two separated laminates, $w_T^{(2)}$ and $w_T^{(3)}$, after multiplying them by their respective volumes. The delamination work is then added to obtain the total work potential,

$$W_T = 2\{w_T^{(1)}(B-a)h^{(1)} + [w_T^{(2)}h^{(2)} + w_T^{(3)}h^{(3)}]a\}L + 2G_c aL \quad (38)$$

where B is the specimen half-width, a is the delamination depth, L is the (assumed) constant delamination length, $h^{(i)}$ are the section thicknesses and G_c is the delamination fracture energy/area. The growth condition is $\partial W_T/\partial a = 0$, which may be written as

$$G = G_c \quad (39)$$

where G is the energy release rate,

$$G = w_T^{(1)}h^{(1)} - w_T^{(2)}h^{(2)} - w_T^{(3)}h^{(3)} \quad (40)$$

This expression was evaluated for two cases guided by the data: (i) the 90° plies are included in $w_T^{(3)}$ (for the inner ply-group) and (ii) the 90° plies are omitted. The second case intersects the horizontal G_c line (G_c = 1 lb/in from double cantilever beam tests) at $\varepsilon_x = 0.007$, while the first one does so at $\varepsilon_x = 0.013$, as shown in Fig. 19. Due to transverse cracks and the axial fiber compression, the 90° plies may lose their ability to resist transverse contraction (possibly due to fiber buckling) thus resulting in early delamination. Figure 19 shows that most of the observed delamination takes place between these predicted values.

Thermal strains and Fig. 12

Thermal strains due to cool-down from the cure at 350F have been neglected. We may introduce them through the b_i, Eq. (16), which can be interpreted as free thermal expansion strains. Clearly, by using $\varepsilon_i - b_i$ in place of ε_i in Eqs. (25) - (33), the effect of thermal strains may be taken into account. It should be noted that the omission of them probably does not explain the differences in E_2 in Fig. 12; these differences may really be due to the effect of the constraint from adjacent plies in reducing microdamage in the angle-ply laminate. It is expected that residual thermal strains in the angle-ply laminate would lead to a lower E_2, rather than a higher value, compared to that for the unidirectional laminates.

CONCLUSIONS

In the simplest form of the theory used here, the unidirectional ply was modeled as a linear elastic material with principal shear and transverse moduli that vary with one scalar parameter (which is equal to the applied work less the strain energy for a unit volume). A modified form of this theory was introduced to account for elastic nonlinearity arising from straining parallel and perpendicular to the fibers (possibly due to initial fiber waviness). Predicted and experimental laminate results for various layups were found to be in good agreement. In order to predict delamination, it was observed that conventional energy release rate analysis may be used, but the work density function replaces strain energy density. Although predictions of unloading and reloading response were not made, a possible approach was described. Viscoelastic behavior was neglected; relatively simple approaches have been proposed elsewhere to account for this behavior at crack tips (4) and in the continuum (10).

ACKNOWLEDGMENT

This research was sponsored by the U.S. Air Force Office of Scientific Research. The author is indebted to Mr. Bob Harbert for doing all of the experimental work and to Mr. Mark Lamborn for developing the data collection and reduction software.

REFERENCES

1. Hahn, H.T. and Tsai, S.W., "Nonlinear Elastic Behavior of Unidirectional Composite Laminae," J. Composite Materials, Vol. 7, Jan. 1973, pp. 102-118.
2. Christensen, R.M., Mechanics of Composite Materials, Wiley, New York, 1979.
3. Sun, C.T. and Chen, J.L., "A Simple Flow Rule for Characterizing Nonlinear Behavior of Fiber Composites," Proc. Sixth Int. Conf. on Composite Materials, Elsevier, London, 1987, pp. 1.250-259.
4. Schapery, R.A., "A Theory of Mechanical Behavior of Elastic Media with Growing Damage and other Changes in Structure," J. Mech. Phys. Solids (in press).
5. Rice, J.R., "Inelastic Constitutive Relations for Solids: An Internal-Variable Theory and its Application to Metal Plasticity," J. Mech. Phys. Solids, Vol. 19, 1971, pp. 433-455.
6. Schapery, R.A., "Deformation and Fracture Characterization of Inelastic Composite Materials Using Potentials," Polymer Eng. Sci., Vol. 27, No. 1, Jan. 1987, pp. 63-76.
7. Lamborn, M.J. and Schapery, R.A., "An Investigation of Deformation Path-Independence of Mechanical Work in Fiber-Reinforced Plastics," Proc. 4th Japan-U.S. Conf. on Composite Materials, Technomic, Lancaster, Pa., 1988, pp. 991-1000.
8. Jones, R.M., Mechanics of Composite Materials, Scripta, Washington D.C., 1975.
9. O'Brien, T.K., "Characterization of Delamination Onset and Growth in a Composite Laminate," Damage in Composite Materials, ASTM STP 775, 1982, pp. 140-167.
10. Schapery, R.A., "On Viscoelastic Deformation and Failure Behavior of Composite Materials with Distributed Flaws," 1981 Advances in Aerospace Structures and Materials - AD-01, ASME, New York, 1981, pp. 5-20.